Spring 1980

Impingement of an axi-symmetric jet on a flat surface

Amir J. Daibes
New Jersey Institute of Technology

IMPINGEMENT OF AN AXI-SYMMETRIC JET ON A FLAT SURFACE

BY

AMIR J. DAIBES

A THESIS

PRESENTED IN PARTIAL FULFILLMENT OF

THE REQUIREMENT FOR THE DEGREE

OF

MASTER OF SCIENCE IN MECHANICAL ENGINEERING

AT

NEW JERSEY INSTITUTE OF TECHNOLOGY

Newark, New Jersey
1980

ABSTRACT

An incompressible, inviscid irrotational flow model was used to represent the normal impingement of a circular axisymmetric jet upon a flat plate. An analytical investigation was conducted to determine the free surface of the jet and the solution of the potential flow problem was obtained using finite difference techniques for jet height-to-nozzle radius ratio of 2.4.

The velocity and pressure distributions at the plate surface and along the jet centerline were obtained.

The results from the finite difference solution are in close agreement with other most recent results from available experimental, and approximate solutions to the potential flow problem.

APPROVAL OF THESIS

IMPINGEMENT OF AN AXI-SYMMETRIC

JET ON A FLAT SURFACE

BY

AMIR J. DAIBES

FOR

DEPARTMENT OF MECHANICAL ENGINEERING

NEW JERSEY INSTITUTE OF TECHNOLOGY

BY

FACULTY COMMITTEE

APPROVED: _____

_____

_____

NEWARK, NEW JERSEY

May, 1980

ACKNOWLEDGEMENT

The author wishes to express his utmost appreciation for the instruction and encouragement of his advisor, Dr. Peter Hrycak. Thanks is also due to Mr. Bengt Holmgren who had given valuable suggestions and consultation during the course of writing the computer program.

Acknowledgement is also due to the Mechanical Engineering Department of New Jersey Institute of Technology for the cooperation given to the author during the period of writing this thesis.

This investigation was partially supported by the Air Force, Contract No. F 33615-79-C 3417.

TABLE OF CONTENTS

page

ABSTRACT i

APPROVAL PAGE ii

ACKNOWLEDGEMENTS iii

TABLE OF CONTENTS iv

LIST OF TABLES vi

LIST OF FIGURES vii

LIST OF SYMBOLS ix

1. INTRODUCTION 1

Uniform Inviscid Impinging Jet Theory 2

Background Literature 3

2. FUNDAMENTAL THEORY 8

Definitions and Basic Equation 8

3. FORMULATION OF THE PROBLEM 13

4. METHOD OF SOLUTION OF THE INTERNAL FLOW PATTERN 17

Graphical Approximation 17

The Finite Difference Method 21

Irregular Stars 24

Sequence of Steps in the Relaxation Solution 25

Computer Program Process 26

5. ANALYSIS OF THE ANALYTICAL RESULTS 29

Velocity Distributions 29

Pressure Distributions 33

Discussion 34

TABLE OF CONTENTS (Continued)

page

CONCLUSIONS 38

RECOMMENDATIONS 39

APPENDIX 41

REFERENCES 53

FIGURES 55

LIST OF TABLES

Table		Page
5.1	Velocity and Pressure Distributions Along Flat Surface . .	30
5.2	Velocity and Pressure Distributions Along the Jet Centerline	31
5.3	Comparison of Velocity Distribution Along Impingement Plane	32

LIST OF FIGURES

Figure		Page
1	Flow Model for Circular Axi-Symmetric Jet Impinging on a Flat Plate	55
2	Graphical Representation of the Nomenclature for the Impinging Jet	56
3	Finite-Difference Representation of an Axisymmetric Jet Impinging on a Flat Plate	57
4	Grid Pattern for the Finite-Difference Solution of the Potential Flow Equation	58
5	a: Regular Square Mesh	59
	b: Laplace Operator Mesh	59
6	Node Notation with Two Equipotential Lines Intercepting All Four Mesh Lines	60
7	Node Notation with Two Equipotential Lines Intercepting All Four Mesh Lines	61
8	Velocity Distribution Along Flat Plate Surface	62
9	Velocity Distribution Along Jet-Centerline	63
10	Static Pressure Distribution Along Flat Plate Surface	64
11	Static Pressure Distribution Along Jet-Centerline	65
12	Radial Velocity and Pressure Distribution of an Axisymmetric Jet Impinging Upon a Flat Plate with a Height-To-Nozzle Radius of 2.4	66
13	Axial Velocity and Pressure Distribution of an Axisymmetric Jet Impinging Upon a Flat Plate with a Height-To-Nozzle Radius Ratio of 2.4	67

LIST OF FIGURES (Continued)

Figure		Page
14	Comparison of Predicted Radial Velocity and Ground Plane Static Pressure Distributions of an Impinging Jet With a Height-To-Nozzle Radius Ratio of 2.4	68
15	Comparison of Predicted Centerline Velocity and Static Pressure Distributions of an Impinging Jet With a Height-To-Nozzle Radius Ratio of 2.4	69
16	Flow Pattern of an Axisymmetric Jet Impinging Upon a Flat Plate	70

LIST OF SYMBOLS

a	constant in Equation (2.12)
D_o	jet diameter
h	fluid depth
h^*	dimensionless distance of straight line connecting the two end points of zero equipotential line
i,j	subscripts in reference to mesh points
n	refers to n^{th} iteration
Po	dynamic pressure at an arbitrary point
Ps	hydrostatic pressure
r	radial coordinate
r^*	dimensionless radial distance from stagnation point
s	tangential distance along free surface
U	velocity component in the r direction
Vo	initial jet velocity
W	velocity component in the axial direction
Z	axial coordinate
z^*	dimensionless axial distance from stagnation point positive upward
z_o	normal distance between target plate and nozzle
ρ	fluid density
ϕ	velocity potential
ψ	Stokes' stream function
θ	the angle, zero equipotential line makes with the plate

CHAPTER 1

Introduction

A class of problems of practical importance are those involving jets. In this class of problems viscous forces are generally confined to small regions of flow, and consequently are of minor importance, so that potential flow theory gives results adequate for most applications. Solutions to these problems have been shown to agree closely with experimental measurements in regions where accelerations and velocities of the flow are relatively high, thus permitting practical applications of the mathematical research in this area. However, potential flow problems involving 3-D free streamlines have proved to be so formidable that researchers have been forced to obtain approximate solutions by numerical techniques or other approximate methods rather than solving the problems in closed form.

The study of jets may be classified into three categories, namely, free jet, impinging jet and wall jet. The free jet, defined as one issuing into unbounded fluid, finds its application in such problems as the mixing and combustion of gaseous or atomized liquid fuel injected into air. It has received attention also in connection with water discharge from a submerged outlet, and discharge of conditioned air into a room. The

impinging jet, a term used when the jet strikes a plane, solid surface in its path at any given angle, finds its chief application in heat transfer processes as in jet cooling of commercial products such as strip steel and plate glass. However the problems associated with jets issuing from rockets or vertical take-off and landing aircraft also belong to this category. The wall jet, which issues tangentially to a plane surface and may, therefore, be regarded as a limiting case of impinging jets with zero angle of impingement, also has its chief application in heat transfer.

Uniform Inviscid Impinging Jet Theory

An inviscid jet in fluid otherwise at rest is in the class of free streamline flows. The essential difficulty in treating such flows analytically lies in the fact that, even though there are well defined boundary conditions on the free streamlines in such flows, the location of the free streamline is not known in advance and must be determined as part of the solution.

There is a considerable body of literature concerning the theory of inviscid jet flows. Exact solutions for two-dimensional inviscid impinging jet flows using hodograph techniques have been obtained, but the available theoretical treatments of inviscid uniform three-dimensional impinging jets are limited to approximate or

numerical methods.

Background Literature On The Potential Jet

The problem of an axisymmetric jet of incompressible, inviscid fluid has been investigated by several authors for certain specified configurations. Apart from the initial study of White[1], in which the essential features of a potential impinging jet were explored, one of the early detailed studies on the problem was carried out by Reich[2]. By utilizing a water jet in an environment of air, as did White, he measured the profile of a large, vertical jet impinging on a horizontal plane. Since the environment for the jet was air, the friction at the free boundary of the jet could be neglected. However, the friction on the impingement plane and the effect of gravity must be taken into consideration.

The first analytical investigation of the potential impinging jet was undertaken by W. Schach[3]. In his study, Schach first assumed the shape of the jet profile and the linear distribution of the velocity potential on the profile. He then re-evaluated the potential distribution on the profile in terms of the originally assumed values through integration of the LaPlace's equation by means of Green's theorem. The resulting distribution was compared with the assumed one, and the profile was

successively modified in the light of the discrepancy between the assumed and computed potential distributions. The process was repeated until the discrepancy became sufficiently small. The primary difficulty with this technique was that no rational basis was derived or shown for correcting the boundary shape.

[4]
Shen obtained an approximate solution for the model of Figure 1 using spherical coordinates, by expanding the velocity potential $\phi\ (r,\theta)$ in series involving spherical harmonics. A finite number of terms in the series are used; boundary conditions are not satisfied identically on the boundaries, but in an average or weighted sense. For example, along boundary BC in Figure 1, the boundary condition is $(\frac{\partial\phi}{\partial S})_{BC} = U_\infty$, where U_∞ is the jet velocity and S is tangent to curve BC. Shen satisfies the condition

$$\int_{\theta_B}^{\theta_C} (\frac{\partial\phi}{\partial S})_{BC} W_i(\theta)d\theta = U_\infty \int_{\theta_B}^{\theta_C} W_i(\theta)d\theta$$

where W_i is a weighting function. If n terms in the series for ϕ are considered, there are n constants to be determined, and, hence n equations like the one above are required. As many equations are obtained as needed by considering different weighting functions, W_i. On boundary BC, the solution obtained is checked by computing the weighted velocity component normal to the boundary. If this condition is satisfied, within the limits of the method, the solution has been obtained. If this condition is not satisfied, a new

boundary must be assumed and the process repeated. Shen indicates a possible iterative technique for obtaining the exact boundary for the flared jet which involves the solution of simultaneous nonlinear algebraic equations, but gives numerical results only for successive approximations type of analysis.

The problem was also investigated more thoroughly by Andre LeClerc.[5] In his study, LeClerc determined the shape of the jet profile by means of an electrical analog employing an electrolyte as a conducting medium for the electric current. The electrolyte was contained in an container shaped in such a way that the electrolyte formed a thin section of the jet sliced by two planes intersecting at the jet axis.

The electrical analogy technique used by LeClerc involves a representation of a body of revolution by such a small segment that the boundary surface need curve in only one plane, and replacement of the usual movable probe by a series of small electrodes precisely located along the boundary.

The electrolyte is thus contained between a sheet of plate glass inclined at perhaps 5 deg. to the horizontal, two vertical copper terminal plates in the approximate form of potential surfaces and well removed

from the zone of measurement, and a strip of plastic at right angles to the glass and formed to represent the curved boundary. The centerline, corresponding to the intersection of the free surface of the electrolyte and the glass plate, is further defined by a low wall of paraffin to eliminate capillary creep. A 0.01 molar solution of copper sulphate with a small admixture of sulphuric acid is used as the electrolyte. The electrodes are formed of 0.015 in. copper wire passing through holes in the plastic strip; the holes are drilled on a precision milling machine, the wires cemented in place, and the contact surfaces polished flush.

An electrical potential is applied between the terminal plates, and the resulting potential difference between each successive pair of boundary electrodes is measured by means of a bridge circuit containing a sensitive null indicator. The potential difference, divided by the electrode spacing, is assumed proportional to the velocity at the mid-point between the electrodes. The curved edge of the container, which corresponded to the free boundary of the jet, was successively adjusted by trial and error until a linear distribution of the voltage drop was obtained along the curved edge of the container.

After the jet profile was determined, LeClerc obtained the potential distribution within the jet numerically by means of the relaxation method. The velocity distribution was obtained subsequently from the potential.

Comparison of the above mentioned studies shows that there is a considerable discrepancy between the jet profiles as obtained by LeClerc and by Schach. The profile obtained by Reich, although it includes the effects of the gravity and the friction on the impingement plane, agrees more closely with LeClerc's. Moreover, the pressure distribution over the impingement plane computed by LeClerc has been verified experimentally by Koumoutsos. [6]

CHAPTER 2

Fundamental Theory

In this chapter the fundamental theory on which the present research is based will be presented.

Some Definitions and Basic Equations. The following definitions and equations, which can be found in most standard text books (e.g. Abramovich [7], Schlichting [8]) are relevant to the present study and hence summarized hereafter for convenience of reference.

Steady flow. A flow whose physical properties such as velocity V, fluid density ρ, and pressure P, at every point in the flow domain do not change with time.

Ideal fluid. A fluid which is both incompressible and inviscid. "Incompressible" means that the fluid occupies a definite volume and is unaffected by change in pressure. "Inviscid" implies the fluid has zero coefficient of viscosity μ and hence offers no resistance to shearing deformations.

Streamline. A continous line drawn through the flow so that it has the direction of the velocity vector $\vec{V}$ at every point on the line. Consequently, no fluid may pass across a streamline. A streamline is mathematically defined by:

$$\vec{V} \times d\vec{S} = 0 \qquad (2.1)$$

or as:

$$Wdr - Udz = 0 \quad \text{for axisymmetric flow} \qquad (2.2)$$

in which S is the tangent at each point on the streamline, W and U are the velocity components in the axial (z) and radial (r) directions, respectively.

Free streamline. A streamline on which the pressure is a constant. For instance, the streamline on the interface of fluid and air of flow issuing forth from a slot or orifice is a free streamline.

Equipotential line. A line on which the fluid particles have the same potential energy. Flow passes an equipotential line at right angles to all points on the line.

Flow net. A net which is composed of two orthogonal sets of lines, streamlines and equipotential lines.

Stream function ψ. A mathematical device used to describe the form of any particular flow, which when:

(a): set equal to constants result in different streamlines in two-dimensional flow, or annular stream surfaces in axisymmetric flow.

(b): differentiated properly yields velocity com-

ponents, i.e.

$$U = \frac{1}{r}\frac{\partial \psi}{\partial z} \qquad W = -\frac{1}{r}\frac{\partial \psi}{\partial r} \quad \text{for axisymmetric flow} \tag{2.3}$$

(c): taking the difference between two streamlines yields the flow rate between these two adjacent stream surfaces.

Velocity potential function ϕ. Another mathematical device, a useful complementary function of ψ, used to describe a flow pattern, which when:

(a): set equal to constants results in velocity potential lines in two-dimensional flow, or velocity potential surfaces in axisymmetric flow.

(b): differentiated with respect to distance in any particular direction yields the velocity in that direction, i.e.

$$U = \frac{\partial \phi}{\partial r} \quad , \quad W = \frac{\partial \phi}{\partial z} \quad \text{for axisymmetric flow} \tag{2.4}$$

(c): gradients are taken gives the velocity field of flow, that is:

$$\vec{V} = \nabla \phi \tag{2.5}$$

It is worth remembering that the stream function exists for both two-dimensional and axisymmetric flow, regardless of whether or not the flow is rotational, while the velocity potential function exists only for

irrotational flow.

Stagnation point. Is a point in the fluid where the velocity is zero. The conditions for stagnation point, where cylindrical coordinates are used and when the flow has axial symmetry, are:

$$U = \frac{\partial \phi}{\partial r} = 0 \quad , \quad W = \frac{\partial \phi}{\partial z} = 0 \tag{2.6}$$

Equations of continuity. The continuity equation simply expresses the law of conservation of mass. When derived in terms of the conventional X,Y,Z rectangular Cartesian coordinate system, the continuity relation may be expressed as:

$$\frac{\partial \rho}{\partial t} + \frac{\partial(\rho U)}{\partial x} + \frac{\partial (\rho V)}{\partial y} + \frac{\partial (\rho W)}{\partial z} = 0 \tag{2.7}$$

or

$$\frac{d\rho}{dt} + \rho \left(\frac{\partial U}{\partial x} + \frac{\partial V}{\partial y} + \frac{\partial W}{\partial z}\right) = 0 \tag{2.8}$$

for any kind of fluid, real or ideal.

For an ideal fluid the rate of change of density following a fluid particle $\frac{d\rho}{dt}$, is zero, and equation (2.8) reduces to:

$$\frac{\partial U}{\partial x} + \frac{\partial V}{\partial y} + \frac{\partial W}{\partial z} = 0 \tag{2.9}$$

In axisymmetric flow the velocity corresponding to the z direction in the Cartesian coordinate system

is zero, then equation (2.9) can be specialized to give:

$$\frac{\partial W}{\partial z} + \frac{1}{r}\frac{\partial}{\partial r}(U\,r) = 0 \quad \text{for axisymmetric flow} \qquad (2.10)$$

The boundary conditions are:

$$z = 0 : U = W = 0 \qquad z = \infty : U = Vo \qquad (2.11)$$

where Vo = initial jet velocity.

For the frictionless case:

$$U = ar \quad ; \quad W = -2az \qquad (2.12)$$

where (a) is a constant. It is seen at once that such a solution satisfies the equation of continuity.

CHAPTER 3

Formulation Of The Problem

Based on the perspective gained from the foregoing survey, the present study was formulated.

The jet considered is a short axisymmetric circular jet impinging normally on a infinite flat plate. The flow region to be analyzed is shown in Figure 2. A cylindrical coordinate system is chosen with Z directed perpendicular to the ground plane, positive outward, and r directed along the ground plane, such that the origin is at the intersection of the ground plane and the axisymmetric jet centerline.

The flow is assumed to be inviscid, incompressible and irrotational. Because of symmetry, the stream function, ψ, and the velocity potential, ϕ, can be defined by:

$$U = \frac{1}{r}\frac{\partial \psi}{\partial z} = \frac{\partial \phi}{\partial r} \tag{3.1}$$

and

$$W = -\frac{1}{r}\frac{\partial \psi}{\partial r} = \frac{\partial \phi}{\partial z}$$

where r is the radial coordinate, z the axial coordinate (as stated above), and U and W are the radial and axial components of fluid velocity, respectively.

The equation of irrotationality in axisymmetric flow

is:

$$\frac{\partial u}{\partial z} - \frac{\partial w}{\partial r} = 0 \qquad (3.3)$$

Substituting Equations (3.1) and (3.2) into Equation (3.3) yields the LaPlace equations.

For the stream function:

$$\frac{\partial^2 \psi}{\partial^2} + \frac{\partial^2 \psi}{\partial z^2} - \frac{1}{r} \frac{\partial \psi}{\partial r} = 0 \qquad (3.4)$$

For the velocity potential:

$$\frac{\partial^2 \phi}{\partial r^2} + \frac{\partial^2 \phi}{\partial z^2} + \frac{1}{r} \frac{\partial \phi}{\partial r} = 0 \qquad (3.5)$$

The differential Equations (3.4) and (3.5) above are the governing equations of the flowfield. The hydrodynamic problem can be considered solved and the flowfield is completely specified if either $\phi(r,z)$ or $\psi(r,z)$ is found.

In addition to Equations (3.4) and (3.5) for ψ and ϕ, there are flow boundary conditions that are required to be satisfied. The boundary conditions applied to the model are as follows:

1. The fluid velocity Vo along the jet's free surface is constant, or equivalently, the pressure is constant along the free surface.

2. On the free surface and at all points on the

boundary, the normal velocity is zero, i.e.

$$\frac{\partial \phi}{\partial n} = 0 \qquad (3.6)$$

where n is the inward normal (into the fluid).

3. The stream function ψ along the centerline of the jet and on the impingement surface is a constant and is set equal to zero.

4. It is assumed that the fluid velocity Vo across the boundaries of the incoming and outgoing flow is constant.

5. The stream function ψ on the free surface is constant.

In the present study the boundary for the incoming flow is established at an axial distance (z) of 2.4 ro from the stagnation point (point of intersection of the r and z axis). The boundary for the outgoing fluid sheet is also at a radial distance (r) of 2.4 ro from the stagnation point. This radial distance of 2.4 times the radius of the impinging jet is considered large, hence the depth (h) of the fluid on the plane is small and the motion is almost radial with velocity Vo, the velocity with which the jet strikes the plane.

The volume rate Q is defined as:

$$Q = \pi r_o^2 Vo \quad \text{(for incoming flow)} \tag{3.7}$$

$$Q = 2\pi rhVo \quad \text{(for outgoing flow)} \tag{3.8}$$

For incompressible, steady flow the continuity equation may take the form

$$Q = \pi r_o^2 Vo = 2\pi rhVo$$

from which the depth of the fluid can be obtained.

$$h = \frac{\pi r_o^2 Vo}{2\pi rVo}$$

or

$$h = \frac{r_o^2}{2r} \tag{3.9}$$

where r again is the radial distance.

In this case the impinging jet radius will be set equal to 1 and thus h = 1/2x2.4 or h = 1/4.8. With this the formulation of the problem is completed.

CHAPTER 4

Method of Solution Of The Internal Flow Pattern

1. Graphical Approximation. The main difficulty involved with the jet impingement flow is that a free surface is present and its position is not originally known and must be found as part of the solution.

A fairly approximate solution of the potential flow problem can be obtained employing a graphical approach. In the present study the graphical method was the fundamental ingredient in approaching the final solution of the problem. Once the centerline axis and the radial axis (along the plate) were drawn and labeled z/r_o and r/r_o respectively (or simply z* and r* in dimensionless form), the fluid depth (h) was drawn as a vertical line of magnitude [h = 1/4.8]*. In extrapolating the profile of the free surface, use is made of the fact that the profile approaches a hyperbola asymptotically as r* increases since the streamlines then become essentially parallel to the impingement plane.

First, from experience, an initial guess as to the location of the free surface is made. It should be noted here that a relatively large graph was used in the early stage of the drawing in attempting a graphical solution to maximize the degree of accuracy required. The next step was to draw additional streamlines, however, the

* Jet radius was taken as unity, see Equation (3.9)

spacing of the streamlines along the fluid depth (h) is uniform because of the fact that at the lower end the velocity is approximately uniform at a given r* parallel to the plate. One can see also that the stream function ψ along the centerline and on the impingement surface is a constant and is set equal to zero. Furthermore, the stream function ψ along the free surface is also a constant and is set equal to 1.

The spacing of streamlines along the incoming stream was determined using the theory of flowrates. Since 2π times the difference in ψ values on the flow surfaces is the flowrate between surfaces, i.e.

$$2\pi\psi = \pi r^2 Vo = Q \tag{4.1}$$

rearranging terms, equation (4.1) is simplified to give

$$\frac{2\psi}{r^2 V_o} = 1 \tag{4.2}$$

where r is the radial distance (proportional to the jet radius r_o) computed along the incoming boundary for each value of the stream function ψ.

A relatively large number of streamlines were drawn, following the guessed free surface. Then the zero equipotential line projected from the stagnation point was drawn intersecting at right angles with all streamlines. On the free surface the boundary condition $\Delta\phi/\Delta S = 1$ was

satisfied by evaluating the values of velocity potential at successive points along the boundary, where S is the distance (proportional to the impinging jet radius r_o) measured along the curve.

On the free streamline the dimensionless velocity potential ϕ/r_oVo was incremented by a constant of 0.1. However, in the "critical area", namely, the area that is close to the zero-equipotential line, the dimensionless velocity potential was incremented by a constant of 0.01.

The end points of the potential lines are now known along the free surface, therefore, the equipotential lines may be drawn with a high degree of precision to satisfy the condition of perpendicularity to the streamlines.

In predicting the end points of equipotential lines near the stagnation point, use was made of the application of the continuity equation in determining the velocity components, i.e. near the stagnation point the following condition occurs:

$$U = ar \quad \text{and} \quad W = -2az \tag{2.12}$$

From this the approximate location of equipotential lines near the stagnation point was obtained along the centerline and along the plate by applying equation (2.4).

Another major contribution as to approaching a graphical solution was extracted from the fact that at axial distances of z/r_o greater than 1.6 the streamlines and equipotential lines were represented as vertical and horizontal lines respectively.*

Based upon the application of all "starting-points" mentioned so far, an initial graphical solution of the flow pattern was obtained using the finite difference technique.

* Previous work done, references [3] & [5]

2. The Finite Difference Method. The essence of the finite difference method involves substitution, for the differential operators in the initial differential equations, of approximate values expressed in terms of differences of the functions at discrete points of the differencing grid. The substitution reduces the problem to the solution of a set of algebraic equations. Although the set of equations may involve a considerable number of unknown quantities, its solution is mathematically easier than that of the original problem. The number of equations and the number of elements in some vector, say ϕ for which a set of difference equations is formulated, correspond to the number of grid intersections or "points" times the number of dependent variables. Generally, the equations are nonlinear, but at each iteration one can think of them as a set of linear algebraic equations.

As a first step in approaching a finite difference solution to the governing LaPlace equation, a grid pattern was formed, as shown in Figure 3, within the space surrounded by the boundary conditions, and at each grid intersection or nodal point the derivatives were replaced by a difference approximation.

In the finite difference method, a square grid was used as illustrated in Figure 4. The origin was arbitrarily

placed at the stagnation point. A successive over relaxation method was employed.

The governing LaPlace differential equation for the potential flow is stated below for convenience of reference.

$$\frac{\partial^2\phi}{\partial r^2} + \frac{\partial^2\phi}{\partial z^2} + \frac{1}{r}\frac{\partial\phi}{\partial r} = 0 \tag{3.5}$$

The finite approximations of the partial derivatives are

$$\frac{\partial\phi_{i,j}}{\partial r} \simeq \frac{\phi_{i+1,j} - \phi_{i-1,j}}{\Delta r^* + \Delta r^*}$$

or (4.3)

$$\frac{\partial\phi_{i,j}}{\partial r} \simeq \frac{\phi_{i+1,j} - \phi_{i-1,j}}{2\Delta r^*}$$

and

$$\frac{\partial^2\phi_{i,j}}{\partial r^2} \simeq \frac{\phi_{i+1,j} - 2\,\phi_{i,j} + \phi_{i-1,j}}{(\Delta r^*)^2} \tag{4.4}$$

similarly

$$\frac{\partial^2\phi_{i,j}}{\partial z^2} \simeq \frac{\phi_{i,j+1} - 2\phi_{i,j} + \phi_{i,j-1}}{(\Delta z^*)^2} \tag{4.5}$$

where i,j subscripts refer to mesh points as shown in Figure 4.

It should be noted here that a square grid denotes that grid spacings in the r and z directions must be

equal. Thus,

$$\Delta r^* = \Delta z^* = h \tag{4.6}$$

Upon replacing Δr^* and Δz^* by the equivalent grid spacing (h), and substituting into Equation (3.5) one obtains after simplification

$$\phi_{i+1,j} + \frac{h}{2r}\ \phi_{i+1,j} + \phi_{i,j+1} + \phi_{i-1,j} - \frac{h}{2r}\ \phi_{i-1,j} + \phi_{i,j-1} - 4\phi_{i,j}$$

$$\simeq h^2\ \left(\frac{\partial^2\phi}{\partial r^2} + \frac{1}{r}\ \frac{\partial\phi}{\partial r} + \frac{\partial^2\phi}{\partial z^2}\right) \tag{4.7}$$

where (r) is the magnitude of radial coordinate of point (i,j).

From Equations (4.7) and (3.5) the residual at any point (i,j) is given by

$$\phi_{i+1,j} + \frac{h}{2r}\ \phi_{i+1,j} + \phi_{i,j+1} + \phi_{i-1,j} - \frac{h}{2r}\ \phi_{i-1,j}$$

$$+ \phi_{i,j-1} - 4\phi_{i,j} = R_{i,j} \tag{4.8}$$

where $R_{i,j}$ for LaPlace equation is zero and, by considering

this and also the residuals at the four surrounding points, the unit dimensionless operator of the velocity potential ϕ at point (i,j) follows

$$\phi_{i,j} = \frac{1}{4}\left[\left(\phi_{i+1,j} + \frac{h}{2r}\,\phi_{i+1,j}\right) + \phi_{i,j+1} + \left(\phi_{i-1,j} - \frac{h}{2r}\,\phi_{i-1,j}\right) + \phi_{i,j-1}\right] \tag{4.9}$$

Referring to the mesh shown in Figure 5b note that a displacement of +1 (or grid spacing h) at point 0 gives a residual at point 1 of amount $1 + \frac{h}{2r}$ and at point 3 of amount 1 - h/2r. Thus, although it is independent of the z coordinate of point 0, the operator is a function of the r coordinate.

Irregular Stars

The effect of a curved boundary on the regular five point finite difference expression is considered here. Due to the non-coincidence of the boundary with the nodal mesh points not all of the mesh arms are of standard length (h). Therefore, special finite difference equations are required where one or more grid lines is intercepted by a boundary of the jet as shown in Figures 6 and 7.

When all four mesh lines are intercepted, the partial derivatives are approximated by

$$\frac{\partial \phi_{i,j}}{\partial r} \simeq \frac{1}{h} \left[\frac{a}{a(a+c)} \phi_A - \frac{a}{c(a+c)} \phi_C + \frac{a-c}{a \cdot c} \phi_{i,j}\right] \tag{4.10}$$

and

$$\frac{\partial^2 \phi_{i,j}}{\partial r^2} \simeq \frac{2}{h^2} \left[\frac{\phi_A}{a(a+c)} + \frac{\phi_C}{c(a+c)} - \frac{\phi_{i,j}}{a \cdot c}\right] \tag{4.11}$$

similarly

$$\frac{\partial^2 \phi_{i,j}}{\partial z^2} \simeq \frac{2}{h^2} \left[\frac{\phi_B}{b(b+d)} + \frac{\phi_D}{d(b+d)} - \frac{\phi_{i,j}}{b \cdot d}\right. \tag{4.12}$$

Equations (4.10) through (4.12) could be specialized after substitution into Equation (3.5) and arrangement of terms to give the eigenvalue of the dimensionless velocity potential ϕ at point (i,j) for the case where equipotential line(s) intercept(s), one, two, three, or all four mesh lines.

Sequence Of Steps In The Relaxation Solution

The solution begins with the approximate eigenvalues of ϕ and known values at the prescribed free streamline obtained from the graphical solution. These values were stored in the computer memory storage to be used as initial values. Then the iterative equation (4.9) was modified to yield

$$\phi_{i,j} \simeq (1 - w)\, \phi_{i,j}^{(n)} + \frac{w}{4} \left[\frac{h}{2r} \phi_{i+1,j}\right. \tag{4.13}$$

$$+ \left(1 - \frac{h}{2r}\right) \phi_{i-1,j} + \phi_{i,j+1} + \phi_{i,j-1}\Big]$$

where (n) and (n + 1) denote two successive iterations, and (w) is the relaxation parameter.

A computer program was written such that Equation (4.13) was used to sweep all the nodal points and to calculate a new set of eigenvalues $\phi_{i,j}$. The sequence used is called a cyclic, single-step process* which is repeated over and over to calculate successively $\phi_{i,j}^{(1)}$, $\phi_{i,j}^{(2)}$, ...etc. One uses in each sweep the known set of dimensionless velocity potentials $\phi_{i,j}^{(n)}$ to calculate a new set of $\phi_{i,j}^{(n+1)}$. Finally, there results

$$\phi_{i,j}^{(n+1)} - \phi_{i,j}^{(n)} \leq e \qquad (4.14)$$

at all nodal points, where (e) is a prescribed value of the error in the velocity potential. When this condition has been met, the iteration has converged to the solution of the finite difference approximation of the LaPlace equation for the specific grid spacing value of (h) used to form the mesh.

Computer Program Process

One of the primary steps taken in writing the computer program was deciding on the number of nodes to be

* This method is known as the Gauss-Seidel method, and when the relaxation parameter (w) is greater than 1 as is the case in the present program, this method is commonly referred to as successive over relaxation or simply SOR.

used. At first, a simple* square 13 x 13 matrix was constructed so that it includes the flow field, with its origin placed at the stagnation point. Nodal points located outside the flowfield were set equal to zero. From the initially assumed values, the computer was operated and its results were obtained after 10 iterations. These new dimensionless velocity potential values were then used to adjust the initially prescribed free streamline and a new graph was drawn. Then new assumed values were extracted graphically and fed to the computer. This process was repeated over 15 times at which the solution was stable.

Experience gained from several tentative solutions obtained during the process of debugging the computer program indicates that convergence does occur fast enough to be practical if a not too coarse a mesh is used.

In order to approach the final analytical solution, the square matrix was augmented to 25 x 25 so that the grid spacing was decreased and finer mesh was obtained. The square mesh was small enough to produce 285 internal nodes with grid spacing of $h = 0.1r_o$. Additional node points are located at all intersections of the grid lines with the plate and with the free streamline.

* Referred to as the Jordan Canonical form matrix.

Again, the values obtained during the last previous iteration were used as initial values. After 10 iterations new values were avaliable. These values, once more were employed for further adjustments of the free surface. The mechanics of re-adjusting the free surface consists of satisfying a necessary boundary condition and that is that a streamline must be everywhere normal to lines of constant velocity potential. Also the tangential derivative $\partial\phi/\partial s$ = constant, is applied at the free stream surface.

The criterion for sufficient relaxation was determined by carrying out an extremely large number of iterations for a fixed boundary shape and finally, on the last run, the velocity potential values at the boundaries were recalculated and 10 last iterations were performed. The change in velocity potential values at that point was less than 0.001% for every node point in the grid, which revealed optimality. The relaxation was ended then and the solution was essentially complete.

Much work has been done on potential axisymmetric flow that impressed the author of this thesis, and which may be helpful to the reader. Although References 9-24 have not been used in the thesis directly, they are still mentioned in the bibliography for convenience. Of help was Lee's work[10] that shows a great deal of similarity with the present solution in the pressure distribution over the plate, illustrating the fact that the potential core flow of viscous fluid has a close physical Ryhmig relation to the flow of ideal fluid. Ryhmig[9] shows an interesting new approach, convenient for axisymmetric systems where the impingement plate has a curvature.

CHAPTER 5

Analysis Of The Analytical Results

1. Velocity Distributions. Once the flowfield generated by the impingement of a circular axisymmetric jet upon a flat plate was specified in terms of the velocity potential as a function of the radial and axial coordinates, i.e. $\phi(r,z)$ respectively, the radial and axial velocities with respect to the initial jet velocity (Vo) may be obtained using the following equations.

$$u = \frac{\partial \phi}{\partial r} \qquad \text{radial velocity} \qquad (3.1)$$

$$w = \frac{\partial \phi}{\partial z} \qquad \text{axial velocity} \qquad (3.2)$$

Equations (3.1) and (3.2) are modified to yield velocity distributions in dimensionless form.

$$\frac{u}{V_o} = \frac{\Delta \phi}{\Delta r^*} \qquad (5.1)$$

where ϕ measured along the plate surface, and similarly

$$\frac{w}{V_o} = \frac{\Delta \phi}{\Delta r^*} \qquad (5.2)$$

where ϕ measured along jet centerline.

Note that if the velocity at point $r^* = 0.3$ was required, one should take ($\Delta\phi$ = at $r^* = 0.4$ - $\Delta\phi$ at $r^* = 0.2$)

and the r* or z* would always be equal to 0.2 ro.

Tabulated results obtained from computer output for the velocity distributions are stated below.

TABLE 5.1

Analytical Velocity and Pressure Distributions Along the Flat Plate Surface for zo/ro = 2.4

$\frac{r}{r_o}$	$\frac{v}{V_o}$	$\frac{P_s - P_o}{\rho V_o^2/2}$
0	0.0000	1.0000
.1	0.0510	0.9973
.2	0.0994	0.9901
.3	0.1538	0.9763
.4	0.1998	0.9600
.5	0.2533	0.9358
.6	0.3111	0.9031
.7	0.3570	0.8725
.8	0.4218	0.8220
.9	0.4727	0.7765
1.0	0.5314	0.7175
1.1	0.5948	0.6461
1.2	0.6492	0.5785
1.3	0.7123	0.4925
1.4	0.7711	0.4053
1.5	0.8225	0.3233
1.6	0.8713	0.2406
1.7	0.9075	0.1763
1.8	0.9335	0.1284
1.9	0.9450	0.1069
2.0	0.9611	0.0762
2.1	0.9701	0.0588
2.2	0.9730	0.5322
2.3	0.9789	0.0415

TABLE 5.2

Analytical Velocity and Pressure Distributions

Along the Jet Centerline for zo/ro = 2.4

(W/Vo is positive upward)

$\frac{z}{r_o}$	$\frac{w}{V_o}$	$\frac{P_s - P_o}{\rho V_o/2}$
0	0.0000	1.0000
.1	0.0762	0.9941
.2	0.1469	0.9784
.3	0.2539	0.9355
.4	0.3305	0.8907
.5	0.3947	0.8442
.6	0.4741	0.7751
.7	0.5230	0.7264
.8	0.5974	0.6430
.9	0.6604	0.5638
1.0	0.7179	0.4845
1.1	0.7567	0.4273
1.2	0.7947	0.3684
1.3	0.8269	0.3162
1.4	0.8568	0.2657
1.5	0.9280	0.1386
1.6	0.9427	0.1112
1.7	0.9478	0.1015
1.8	0.9692	0.0605
1.9	0.9848	0.0301
2.0	0.9933	0.0132
2.1	0.9973	5.3899×10^{-3}
2.2	0.9991	1.7966×10^{-3}
2.3	0.9998	2.6388×10^{-4}

TABLE 5.3

Velocity Distribution on the Impingement Plane

Due to a Potential Impinging Jet.

$\frac{r}{r_o}$	Present Study	LeClerc
0.0	0.0	0.0
0.1	0.0510	0.050
0.2	0.0994	0.100
0.3	0.1538	1.151
0.4	0.1998	0.202
0.5	.2533	0.254
0.6	.3111	0.307
0.7	.3570	0.362
0.8	.4218	0.417
0.9	.4727	0.474
1.0	.5314	0.532
1.1	.5948	0.591
1.2	.6492	0.651
1.3	.7123	0.711
1.4	.7711	0.770
1.5	.8225	0.824
1.6	.8713	0.871
1.7	.9075	0.908
1.8	.9335	0.933
1.9	.9450	0.945
2.0	.9611	0.961
2.1	0.9701	0.968
2.2	.9730	0.973
2.3	.9789	0.976

2. Pressure Distribution. In potential flow problems the pressure distribution is given by Bernoulli's equation. If Ps denotes the hydrostatic or simply the stagnation pressure and Po is the dynamic pressure at an arbitrary point, hence for potential flow

$$P_s = P_o + \frac{\rho V_o^2}{2} \left[1 - \left(\frac{U}{V_o}\right)^2\right] \tag{5.3}$$

or

$$\frac{P_s - P_o}{\rho V_{o/2}^2} = 1 - \left(\frac{U}{V_o}\right)^2 \tag{5.4}$$

similarly

$$\frac{P_s - P_o}{\rho V_{o/2}^2} = 1 - \left(\frac{W}{V_o}\right)^2 \tag{5.5}$$

where ρ is the fluid density and Vo is the jet velocity.

The pressure distribution along the flat plate surface was obtained using Equation (5.4), while the distribution along the jet centerline was obtained employing Equation (5.5), analytical results are included in Tables 5.1 and 5.2.

The velocity and pressure distributions obtained from the present study are represented graphically in Figures 8 through 13 and the flow pattern of the impinging jet is presented in Figure 16.

Analysis Of Radial Velocity And Pressure Distributions

The velocity variation along the flat plate is presented in Figure 8. It is readily seen that the radial velocity increases manotonically and linearly at first from zero at the stagnation point to a region where r/ro is smaller than 1.6. Beyond this region the rate of increase decreases drastically where in the case of flow of real fluid the velocity begins to decay due to energy dissipation.

Numerical results obtained from present study for the velocity distribution on the impingement plane, and those obtained by LeClerc[5] are included in Table 5.3. This Table is presented graphically in Figure 14. Comparison between the two mentioned results, reveals similarity within the range covering $0 \leq r/ro \leq 0.6$. Also, close agreement prevailed when $r/ro \geq 1.2$. However, for $0.6 \leq r/ro \leq 1.2$ some minor discrepancy occured. This said discrepancy is primarily due to the difference in the shape of the free stream surface obtained in the present case.

Further comparison, concerning the radial velocity obtained from the finite difference method, was made with the available published work of Schach. Aside from the fact that difficulty was exercised in extracting Schach's velocity distribution from a very small graph in his

article, it was found that there was some qualitative agreement between the two results for short radial distances from the stagnation point, but for the range $0.5 \leq r/r0 \leq 1.7$ the rate of increase of the radial velocity corresponding to the present analysis was noticeably less than that obtained by Schach, however the opposite of the latter case occurs for $1.6 \leq r/ro \leq 2.4$. This result is shown in Figure 14.

Since the pressure along the flat plate was calculated in dimensionless form using Bernoulli's equation, it is then clearly seen from Equation (5.3) that the pressure distribution is totally dependent on the corresponding velocity distribution. Hence, it is fairly obvious that the pressure distribution obtained by LeClerc will be or in fact is similar to the present results as shown in Figure 14, within the range where velocity distributions were proven to be similar. By the same 'token', within the range where $0.6 \leq r/ro \leq 1.2$ the pressure distribution curve obtained here tends to show a decrease at a slightly higher rate than that predicted by LeClerc.

As shown in Figure 14, the pressure distribution obtained by Schach reveals that the hydrostatic pressure tends to reach the dynamic (ambient) pressure at a faster rate for radial distances of $r \leq 1.7$; beyond this

point the slope begins to taper off, and the stagnation pressure peaks up at a farther radial distance than that predicted by the present study.

Further comparison was also made with the experimental results obtained by Lee.[10] Although the nozzle height-to-radius ratio (ro/zo) of that employed by Lee was different from the one assumed in the present case, some pronounced agreement was sought even though theory asserts that real jets, encounter a free-mixing zone prior to entry into the impingement region. The presence of mixing zone, compressibility and viscosity in real jets employed in experiments, tend to maximize the rate at which the velocity is decreasing, and therefore higher normalized pressures are expected near the stagnation point.

Analysis Of Centerline Velocity And Pressure Distributions

For normal axisymmetric jet impingement, Schlichting[8] and many others, express the criterion that the impingement region commences when the centerline velocity is 98% of that in the undisturbed free jet at the identical distance from the nozzle exit. According to the present computations, the location of this point is at $z/ro \simeq 1.9$, which is in close agreement with the value $z/ro \simeq 2.0$ observed by Schlichting. Schach found that this point at which impingement region begins where the ground effect is

first felt is at an axial distance of $z/ro \simeq 2.3$ which is in conflict with the above mentioned theory. It is worth mentioning here that LeClerc's results are comparable to those obtained by the present study.

Based on the previous discussion, one can already see the similarity that exists in centerline velocity distribution between the results obtained by the finite difference method and those obtained by LeClerc for the region where $z/ro > 2.2$. However, for axial distances of $1.4 \leq z/ro \leq 1.8$ the velocity distributions obtained here tend to follow Schach's prediction more closely than LeClerc's.

Near the stagnation point, the velocity distribution was found to be comparable in both cases as shown in Figure 15. The distribution of pressure along the jet centerline compared with LeClerc's and Schach's is shown in Figure 15. The agreement between the current computations and those of LeClerc's is obvious for the region $z/ro \leq 1.4$. However, beyond this point it was found based on thorough analysis that the current curve is steeper and the static pressure at an axial distance of $z/ro > 1.4$ tends to approach the dynamic pressure. This is a considerable improvement upon the distribution of LeClerc which breaks down at large distances from the stagnation point.

CONCLUSIONS

Though the equations for axisymmetric jet impingement on flat surfaces are not integrable in a closed form, the use of a finite difference potential flow analysis combined with initial graphical approximations appears to be a fairly flexible computational technique for handling problems of jet impingement. This technique produced good agreement with results of other investigators using different techniques, which were available from the literature on axisymmetric jets.

A free surface consisting of a streamline or any arbitrarily-shaped solid surface can be handled with no major difficulty by the finite difference method. The limitations of this approach are, however, that the flow be laminar and that no regions of separated flow exist.

The accuracy of the prediction of velocity potential in the flow region, from which velocity components and pressure distributions were extracted by using this technique, proved to be reasonably good and in some respects resulted in a substantial improvement of the predictions obtained by the more time consuming methods.

RECOMMENDATIONS

Although the solution of the potential flow problem investigated in the present study is complete, there are still some areas in heat transfer and fluid mechanics that future studies should include in the applicability of the finite difference technique. Some of the recommended areas are stated as follows:

1. Heat transfer distribution on a flat plate produced by the impingement of an axisymmetric jet.

2. With appropriate modifications the technique has the potential of analyzing a large class of problems involving phase change where the shape of the heat transfer surface and the distribution of heat transfer on it are co-determined.

3. It would be most interesting to include the solution of the integral boundary layer which requires as an input the free stream velocity and its first derivative along the impingement surface. Since these parameters are calculated by a numerical differentiation of the finite difference solution for the potential flow, a high degree of accuracy and smoothness of these

results are required. This factor, therefore, will be expected to control the finite difference nodal spacing required in regions of rapidly varying velocity.

One of the main expected numerical difficulties with this technique when applied to the latter case would involve the matching of the solutions between the potential flow and the boundary layer regions.

APPENDIX

Computer Program

The computer program was written in BASIC language, which makes it easier for engineers who are not acquainted with computer programming to relate to the subject. The computer program is included in the next few pages. Also included, is the computer input, that is the initial velocity potential values used on the last run. Then the new values of the velocity potential computed follow. From the predicted flow pattern, the velocity and pressure distribution along the flat plate, and along the jet centerline were computed and tabulated results are located in the back of the Appendix.

```
]RENUMB A:AT

]LIST

10  DIM A(24,24),B(24,24)
20  DATA 0,.001014,.010016,.02196,.04022,.06256,.09105,.12416,.16345,.20766,.25825,.31406
30  DATA .37645,.44426,.51865,.59826,.68345,.77226,.86505,.96086,1.06405,1.15107,1.26207,1.34567,1.44367
40  DATA -.005,-.001,.007,.01,.033,.048,.089,.111,.156,.194,.253,.301
50  DATA .367,.435,.511,.586,.671,.765,.852,.949,1.057,1.143,1.245,1.343,0.0
60  DATA -.015,-.012,-.001,.003,.013,.041,.072,.098,.139,.17,.233,.281
70  DATA .346,.418,.492,.57,.656,.748,.846,.938,1.038,1.135,1.236,1.335,1.445
80  DATA -.035,-.031,-.026,-.009,.002,.016,.039,.062,.103,.148,.198,.250
90  DATA .318,.382,.467,.544,.633,.729,0,0,0,0,0,0,0
100  DATA -0.065,-0.061,-0.055,-0.050,-0.038,-0.021,.01,.043,.075,.109,.157,.201
110  DATA .273,.342,.416,0,0,0,0,0,0,0,0,0,0
120  DATA -.102,-.099,-.092,-.089,-.081,-.055,-.022,-.001,.020,.064,.109,.152
130  DATA .212,.281,0,0,0,0,0,0,0,0,0,0,0
140  DATA -.145,-.141,-.136,-.132,-.124,-.102,-.087,-.061,-.034,.005,.043,.084
150  DATA .143,0,0,0,0,0,0,0,0,0,0,0,0
160  DATA -.197,-.194,-.189,-.183,-.177,-.163,-.145,-.123,-.096,-.069,-.031,.009
170  DATA 0,0,0,0,0,0,0,0,0,0,0,0,0
180  DATA -.252,-.249,-.241,-.238,-.233,-.227,-.218,-.185,-.174,-.143,-.118,-.079
190  DATA 0,0,0,0,0,0,0,0,0,0,0,0,0
200  DATA -.317,-.314,-.308,-.301,-.298,-.295,-.289,-.271,-.252,-.229,-.205,0
210  DATA 0,0,0,0,0,0,0,0,0,0,0,0,0
220  DATA -.386,-.382,-.377,-.368,-.367,-.362,-.359,-.355,-.354,-.336,-.299,0
230  DATA 0,0,0,0,0,0,0,0,0,0,0,0,0
240  DATA -.461,-.453,-.451,-.447,-.441,-.439,-.433,-.431,-.426,-.410,-.396,0
250  DATA 0,0,0,0,0,0,0,0,0,0,0,0,0
260  DATA -.538,-.536,-.530,-.528,-.526,-.524,-.521,-.518,-.516,-.513,-.489,0
270  DATA 0,0,0,0,0,0,0,0,0,0,0,0,0
280  DATA -.620,-.616,-.609,-.607,-.605,-.602,-.601,-.600,-.598,-.597,-.595,0
290  DATA 0,0,0,0,0,0,0,0,0,0,0,0,0
300  DATA -.703,-.698,-.697,-.696,-.694,-.691,-.689,-.687,-.685,-.684,-.684,0
310  DATA 0,0,0,0,0,0,0,0,0,0,0,0,0
320  DATA -.791,-.789,-.786,-.785,-.784,-.784,-.783,-.782,-.781,-.780,-.779,0
330  DATA 0,0,0,0,0,0,0,0,0,0,0,0,0
340  DATA -.882,-.882,-.882,-.881,-.881,-.881,-.88,-.88,-.88,-.88,-.88,0
350  DATA 0,0,0,0,0,0,0,0,0,0,0,0,0
360  DATA -.973,-.973,-.973,-.973,-.972,-.972,-.972,-.972,-.971,-.971,-.970,0
370  DATA 0,0,0,0,0,0,0,0,0,0,0,0,0
380  DATA -1.07,-1.07,-1.07,-1.07,-1.07,-1.07,-1.07,-1.069,-1.069,-1.069,-1.069,0
390  DATA 0,0,0,0,0,0,0,0,0,0,0,0,0
400  DATA -1.169,-1.169,-1.169,-1.169,-1.169,-1.169,-1.169,-1.169,-1.169,-1.169,-1.169,0
410  DATA 0,0,0,0,0,0,0,0,0,0,0,0,0
420  DATA -1.27,-1.27,-1.27,-1.27,-1.27,-1.27,-1.27,-1.27,-1.27,-1.27,-1.27,0
430  DATA 0,0,0,0,0,0,0,0,0,0,0,0,0
440  DATA -1.37,-1.37,-1.37,-1.37,-1.37,-1.37,-1.37,-1.37,-1.37,-1.37,-1.37,0
450  DATA 0,0,0,0,0,0,0,0,0,0,0,0,0
460  DATA -1.47,-1.47,-1.47,-1.47,-1.47,-1.47,-1.47,-1.47,-1.47,-1.47,-1.47,0
470  DATA 0,0,0,0,0,0,0,0,0,0,0,0,0
480  DATA -1.57,-1.57,-1.57,-1.57,-1.57,-1.57,-1.57,-1.57,-1.57,-1.57,-1.57,0
490  DATA 0,0,0,0,0,0,0,0,0,0,0,0,0
500  DATA -1.67,-1.67,-1.67,-1.67,-1.67,-1.67,-1.67,-1.67,-1.67,-1.67,-1.67,0
510  DATA 0,0,0,0,0,0,0,0,0,0,0,0,0
1000  FOR I = 0 TO 24
1010  FOR J = 0 TO 24
1020  READ A(I,J)
```

```
1080  NEXT J
1090  NEXT I
1100  FOR I = 0 TO 24
1101  FOR J = 0 TO 24
1102 B(I,J) = A(I,J)
1103  NEXT J
1104  NEXT I
1105  GOSUB 9000
1106  FOR K = 1 TO 10
1107 C1 = 1
1108 C5 = .05
1110  FOR I = 23 TO 1 STEP  - 1
1120  FOR J = 1 TO 23
1170 R0 = .1 * J
1200 Q1 = A(I,J + 1)
1210 Q2 = A(I + 1,J)
1220 Q3 = A(I,J - 1)
1230 Q4 = A(I - 1,J)
1240  IF Q1 = 0 THEN 1500
1250  IF Q2 = 0 THEN 1500
1260  IF Q3 = 0 THEN 1500
1270  IF Q4 = 0 THEN 1500
1280 B(I,J) = (Q1 + (C5 * Q1 / R0) + Q2 + Q3 - (Q3 * C5 / R0) + Q4) / 4
1500  NEXT J
1510  NEXT I
1520  FOR I = 23 TO 1 STEP  - 1
1530  FOR J = 1 TO 23
1535  IF B(I,J) = 0 THEN 1550
1540 A(I,J) = B(I,J)
1550  NEXT J
1560  NEXT I
1562  PRINT "ITERATION ";K
1564  NEXT K
1566  GOSUB 2000
1570  GOSUB 9000
1580  PRINT D$;"PR#1"
1585  PRINT ""
1590  PRINT "R0","V","P"
1600  PRINT
1610  FOR J = 1 TO 23
1620 V = (B(0,J + 1) - B(0,J - 1)) / .2
1630 P = 1 - V ^ 2
1640  PRINT J / 10,V,P
1650  NEXT J
1660  FOR I = 1 TO 42
1670  PRINT " "
1680  NEXT I
1690  PRINT "Z","V","P"
1700  PRINT
1710  FOR I = 1 TO 23
1720 V = (B(I + 1,0) - B(I - 1,0)) / .2
1730 P = 1 - V ^ 2
1740  PRINT I / 10,V,P
1750  NEXT I
1760  PRINT D$;"PR#0"
1770  END
2000  FOR I = 24 TO 16 STEP  - 1
2010 B(I,0) = B(I,1)
```

1780 END
2000 FOR I = 24 TO 16 STEP -1
2010 B(I,0) = B(I,1)
2030 FOR I = 15 TO 1 STEP -1

```
2030  FOR I = 15 TO 1 STEP  - 1
2040 Q1 = B(I,2)
2050 Q2 = B(I + 1,1)
2060 Q4 = B(I - 1,1)
2070 Q0 = B(I,1)
2080 B(I,0) = 8 * Q0 - 3 * Q1 - 2 * Q2 - 2 * Q4
2090  NEXT I
2100  FOR J = 1 TO 22
2110 R0 = .1 * J
2120 Q0 = B(1,J)
2130 Q1 = B(1,J + 1)
2140 Q2 = B(2,J)
2150 Q3 = B(1,J - 1)
2160 B(0,J) = 4 * Q0 - Q1 * (1 + (C5 / R0)) - Q2 - Q3 * (1 - (C5 / R0))
2170  NEXT J
2180  RETURN
9000 D$ = ""
9010  PRINT D$;"PR#1"
9015  PRINT ""
9020  PRINT ""
9030  FOR I = 24 TO 0 STEP  - 1
9040  FOR J = 0 TO 7
9050  PRINT B(I,J),;
9060  NEXT J
9075  PRINT : PRINT
9080  NEXT I
9085  GOSUB 9300
9090  FOR I = 24 TO 0 STEP  - 1
9100  FOR J = 8 TO 15
9110  PRINT B(I,J),;
9120  NEXT J
9130  PRINT : PRINT
9140  NEXT I
9142  GOSUB 9300
9145  GOSUB 9200
9147  GOSUB 9300
9150  PRINT D$;"PR#0"
9160  RETURN
9200  FOR I = 24 TO 0 STEP  - 1
9210  FOR J = 16 TO 23
9220  PRINT B(I,J),;
9230  NEXT J
9240  PRINT : PRINT
9250  NEXT I
9260  RETURN
9300  FOR I = 1 TO 16
9310  PRINT " "; NEXT I
9320  RETURN
```

PROU

-1.67	-1.67	-1.67	-1.67	-1.67	-1.67	-1.67	-1.67
-1.57	-1.57	-1.57	-1.57	-1.57	-1.57	-1.57	-1.57
-1.47	-1.47	-1.47	-1.47	-1.47	-1.47	-1.47	-1.47
-1.37	-1.37	-1.37	-1.37	-1.37	-1.37	-1.37	-1.37
-1.27	-1.27	-1.27	-1.27	-1.27	-1.27	-1.27	-1.27
-1.169	-1.169	-1.169	-1.169	-1.169	-1.169	-1.169	-1.169
-1.07	-1.07	-1.07	-1.07	-1.07	-1.07	-1.07	-1.069
-.973	-.973	-.973	-.973	-.972	-.972	-.972	-.972
-.882	-.882	-.882	-.881	-.881	-.881	-.88	-.88
-.791	-.789	-.786	-.785	-.784	-.784	-.783	-.782
-.703	-.698	-.697	-.696	-.694	-.691	-.689	-.687
-.62	-.616	-.609	-.607	-.605	-.602	-.601	-.6
-.539	-.536	-.53	-.528	-.526	-.524	-.521	-.518
-.461	-.453	-.451	-.447	-.441	-.439	-.433	-.431
-.386	-.382	-.377	-.369	-.367	-.362	-.359	-.355
-.317	-.314	-.308	-.301	-.298	-.295	-.289	-.271
-.252	-.249	-.241	-.238	-.233	-.227	-.218	-.185
-.197	-.194	-.189	-.183	-.177	-.163	-.145	-.123
-.145	-.141	-.136	-.132	-.124	-.102	-.087	-.061
-.102	-.099	-.092	-.089	-.081	-.055	-.022	-1E-03
-.065	-.061	-.055	-.05	-.038	-.021	.01	.043
-.035	-.031	-.028	-9E-03	2E-03	.016	.039	.062
-.015	-.012	-1E-03	3E-03	.013	.041	.072	.099
-5E-03	-1E-03	7E-03	.01	.033	.049	.089	.111
0	1.014E-03	.010016	.02196	.04022	.06256	.09105	.12416

-1.67	-1.67	-1.67	0	0	0	0	0
-1.57	-1.57	-1.57	0	0	0	0	0
-1.47	-1.47	-1.47	0	0	0	0	0
-1.37	-1.37	-1.37	0	0	0	0	0
-1.27	-1.27	-1.27	0	0	0	0	0
-1.169	-1.169	-1.169	0	0	0	0	0
-1.069	-1.069	-1.069	0	0	0	0	0
-.971	-.971	-.97	0	0	0	0	0
-.88	-.88	-.88	0	0	0	0	0
-.781	-.78	-.779	0	0	0	0	0
-.685	-.684	-.684	0	0	0	0	0
-.598	-.597	-.595	0	0	0	0	0
-.516	-.513	-.489	0	0	0	0	0
-.426	-.41	-.396	0	0	0	0	0
-.354	-.336	-.299	0	0	0	0	0
-.252	-.229	-.205	0	0	0	0	0
-.174	-.143	-.118	-.079	0	0	0	0
-.096	-.069	-.031	9E-03	0	0	0	0
-.034	5E-03	.043	.084	.143	0	0	0
.028	.064	.109	.152	.212	.281	0	0
.075	.109	.157	.201	.273	.342	.416	0
.103	.148	.198	.25	.318	.392	.467	.544
.139	.17	.233	.281	.346	.418	.492	.57
.156	.194	.253	.301	.367	.435	.511	.586
.16345	.20766	.25825	.31406	.37645	.44426	.51865	.59026

0	0	0	0	0	0	0	0
0	0	0	0	0	0	0	0
0	0	0	0	0	0	0	0
0	0	0	0	0	0	0	0
0	0	0	0	0	0	0	0
0	0	0	0	0	0	0	0
0	0	0	0	0	0	0	0
0	0	0	0	0	0	0	0
0	0	0	0	0	0	0	0
0	0	0	0	0	0	0	0
0	0	0	0	0	0	0	0
0	0	0	0	0	0	0	0
0	0	0	0	0	0	0	0
0	0	0	0	0	0	0	0
0	0	0	0	0	0	0	0
0	0	0	0	0	0	0	0
0	0	0	0	0	0	0	0
0	0	0	0	0	0	0	0
0	0	0	0	0	0	0	0
0	0	0	0	0	0	0	0
0	0	0	0	0	0	0	0
.633	.729	0	0	0	0	0	0
.656	.748	.846	.938	1.039	1.135	1.236	1.335
.671	.765	.852	.949	1.057	1.143	1.245	1.343
.68345	.77226	.86505	.95886	1.05405	1.15107	1.24807	1.34567

PR#0

-1.67	-1.67	-1.67	-1.67	-1.67	-1.67	-1.67	-1.67
-1.56999731	-1.56999731	-1.56999462	-1.56999428	-1.56998925	-1.56998098	-1.56998276	-1.56998115
-1.47002639	-1.47002639	-1.47003715	-1.47002878	-1.47002868	-1.47000993	-1.47000775	-1.4699988
-1.37017706	-1.37017706	-1.37020939	-1.3702292	-1.37019495	-1.37018719	-1.37013329	-1.37010938
-1.27056611	-1.27056611	-1.27075738	-1.2707491	-1.27074997	-1.27065115	-1.27060032	-1.27045149
-1.17150611	-1.17150611	-1.17190208	-1.17202113	-1.17188767	-1.17181208	-1.17158333	-1.17136098
-1.07360323	-1.07360323	-1.07431327	-1.07425453	-1.0741745	-1.07384878	-1.07359689	-1.07311119
-.977658494	-.977658494	-.978150394	-.97816654	-.977713979	-.977369406	-.976786535	-.976195737
-.884025889	-.884025889	-.884285681	-.883726548	-.88324072	-.882411554	-.881674767	-.880719224
-.789114687	-.792849539	-.792427729	-.791829555	-.790674481	-.789652716	-.788274281	-.786774861
-.698406723	-.704173329	-.703658104	-.702250143	-.700950011	-.699061476	-.697119892	-.694642751
-.61773646	-.619153258	-.617658881	-.616149997	-.613788252	-.611464365	-.608177995	-.604453381
-.533023517	-.537083153	-.535581602	-.532993288	-.530398134	-.526395021	-.522073821	-.515972314
-.458795052	-.459295192	-.456929883	-.454246425	-.449877406	-.44529887	-.439162032	-.430274318
-.381671072	-.395305265	-.383062951	-.378932405	-.374273013	-.366646011	-.358552441	-.346348599
-.315208501	-.316495904	-.313493134	-.309124529	-.301772064	-.293737451	-.280936892	-.267529762
-.24958926	-.252834399	-.249681559	-.243530905	-.235048167	-.223514166	-.210446252	-.199007723
-.195719746	-.195524723	-.191379726	-.184675264	-.173886121	-.161490926	-.14278796	-.123107089
-.144987621	-.144335029	-.139604761	-.131274621	-.12014747	-.103500814	-.0850783906	-.0594320756
-.100890162	-.0999144419	-.0946109084	-.0855986028	-.0719278407	-.055372135	-.0322964289	-6.74772164E-03
-.0660470972	-.0620612951	-.0569511855	-.046804139	-.032882594	-.0131808538	9.65827622E-03	.0392317523
-.0347858997	-.0334804116	-.0271902171	-.0165930178	-7.72371908E-04	.0187602038	.0446645171	.0744531029
-.0152545549	-.0127820757	-5.93912081E-03	5.72507833E-03	.0215995885	.0433454473	.0691700572	.1012183
-5.39540473E-03	-1.12538247E-03	6.6428321E-03	.0185099127	.0358884167	.0575809767	.0852653333	.117661096
0	1.014E-03	.0102080952	.0209080597	.0409793058	.0608870177	.0916425271	.123122708

-1.67	-1.67	-1.67	0	0	0	0	0
-1.56998294	-1.5699902	-1.57	0	0	0	0	0
-1.46998751	-1.46998432	-1.47	0	0	0	0	0
-1.37004559	-1.370009	-1.37	0	0	0	0	0
-1.27039489	-1.27007711	-1.27	0	0	0	0	0
-1.17091813	-1.17021696	-1.169	0	0	0	0	0
-1.07244745	-1.07118907	-1.069	0	0	0	0	0
-.975251753	-.973666503	-.97	0	0	0	0	0
-.879710695	-.878900149	-.88	0	0	0	0	0
-.78495537	-.782608596	-.779	0	0	0	0	0
-.691719029	-.68839448	-.684	0	0	0	0	0
-.600030684	-.595807535	-.595	0	0	0	0	0
-.508881553	-.500188823	-.489	0	0	0	0	0
-.419626291	-.408042606	-.396	0	0	0	0	0
-.333172605	-.316550712	-.299	0	0	0	0	0
-.248625326	-.228531284	-.205	0	0	0	0	0
-.170449751	-.143611333	-.114242251	-.079	0	0	0	0
-.0960420907	-.0669356435	-.0311354808	9E-03	0	0	0	0
-.0317775176	3.25012869E-03	.0424506924	.0888606346	.143	0	0	0
.0259562862	.0625936918	.106200713	.156236317	.21416624	.281	0	0
.0728859424	.112691052	.150589529	.211248151	.271390974	.339534086	.416	0
.110591067	.152148144	.199818157	.254300275	.315638112	.384137193	.460340245	.549
.138238169	.181139789	.230210002	.285571427	.347453738	.416183825	.49123433	.572943837
.155986528	.199864799	.249641011	.305519419	.367717828	.435913778	.510635908	.590846828
.163044317	.207488843	.257587093	.31378028	.37655128	.4436207	.519015375	.597851038

0	0	0	0	0	0	0	0
0	0	0	0	0	0	0	0
0	0	0	0	0	0	0	0
0	0	0	0	0	0	0	0
0	0	0	0	0	0	0	0
0	0	0	0	0	0	0	0
0	0	0	0	0	0	0	0
0	0	0	0	0	0	0	0
0	0	0	0	0	0	0	0
0	0	0	0	0	0	0	0
0	0	0	0	0	0	0	0
0	0	0	0	0	0	0	0
0	0	0	0	0	0	0	0
0	0	0	0	0	0	0	0
0	0	0	0	0	0	0	0
0	0	0	0	0	0	0	0
0	0	0	0	0	0	0	0
0	0	0	0	0	0	0	0
0	0	0	0	0	0	0	0
0	0	0	0	0	0	0	0
0	0	0	0	0	0	0	0
.633	.729	0	0	0	0	0	0
.659821506	.751589546	.846	.938	1.039	1.135	1.236	1.335
.676430049	.766043487	.858665774	.952400666	1.0490848	1.14604978	1.24439912	1.343
.683533482	.772128706	.865042356	.958841062	1.05404754	1.15106484	1.24807055	1.34567

PR#0

R0	V	P
.1	.0510404758	.99739487
.2	.0994702987	.99010566
.3	.153856053	.976328315
.4	.19909479	.960042073
.5	.253316106	.93583095
.6	.311178451	.903167972
.7	.357008951	.872544609
.8	.421830674	.822058883
.9	.472713878	.776541589
1	.531457189	.717553256
1.1	.594820937	.646188053
1.2	.6492021	.578536633
1.3	.712320474	.492599542
1.4	.771151694	.405325065
1.5	.822590532	.323344815
1.6	.871388334	.240682371
1.7	.907544369	.176363217
1.8	.93356178	.128462402
1.9	.945025912	.106926025
2	.9611189	.0762504584
2.1	.970115059	.0588767725
2.2	.973025793	.053220805
2.3	.97899725	.0415643848

Z	W	P
.1	-.0762732745	.994182388
.2	-.146952475	.97840497
.3	-.253962211	.935503195
.4	-.33052131	.890755663
.5	-.394702621	.844209841
.6	-.474147923	.775183747
.7	-.523008192	.726462431
.8	-.597443773	.643060938
.9	-.660409058	.563859875
1	-.717932754	.40457256
1.1	-.756762229	.427310928
1.2	-.794707042	.368440717
1.3	-.826916028	.316209882
1.4	-.856891135	.265737583
1.5	-.928095831	.138638129
1.6	-.942719035	.11128082
1.7	-.947886715	.101510776
1.8	-.969238103	.0605774982
1.9	-.984814395	.0301406063
2	-.993354707	.0132464258
2.1	-.997301401	5.38991616E-03
2.2	-.999101272	1.79664764E-03
2.3	-.999868046	2.63889686E-04

REFERENCES

1. White, W.M., "Pitot Tube; Its Formula", Journal of the Association of Engineering Societies, 272, 1901, pp. 35-79.

2. Reich, F., "Umlenkung eines freien Flussigkeits-strahles an einer senkrecht zur Stromungrichtung stehenden ebenen Platte", VDI Forschungsheft, 290, 1926.

3. Schach, W., "Umlenkung eines Kreisformigen Flussig-keitsstrahles an einer ebenen Platte senkrecht zur Stromungsrichtung", Ingenieur Archiv, 6, 1935, pp. 51-59.

4. Shen, Y.C., "Theoretical Analysis of Jet Ground Plane Interaction", IAS Paper No. 62-144, 1962.

5. LeClerc, A., "Deflection of a Liquid Jet by a Per-pendicular Boundary", M.S. Thesis, State University of Iowa, 1948.

6. Koumoutsos, N.G., "Pressure Distribution on a Plane Surface under Normal Impingement of an Axisymmetric Jet", M.S. Thesis, Illinois Institute of Technology, 1959.

7. Abramovich, G.N., "The Theory of Turbulent Jets", MIT Press, Cambridge, Mass., 1963.

8. Schlichting, H., "Boundary Layer Theory", 6th ed., McGraw-Hill Book Company, New York, 1968.

9. Ryhming, I.L., "An Approximate Solution of the Steady Jet Impact Problem", Institut CERAC SA., Ecublens, Journal of Applied Mathematics and Physics (ZA MP), 25, 1974, pp. 515-531.

10. Lee, D.T.H., "Experimental Investigation of Submerged, Incompressible, Turbulent, Impinging Jets", M.S. Thesis, New Jersey Institute of Technology, 1969.

11. Southwell, R. & Vaisey, G., "Relaxation Methods Applied to Engineering Problems", XII, Fluid motions characterized by free streamlines, Phil. Trans. Roy. Soc. London., A 240, 1948, pp. 117-161.

12. Rouse, H. & Abul-Fetouh, A., "Characteristics of Irrotational Flow Through Axially Symmetric Orifice", J. Appl. Mech., 17, 1950, pp. 421-426.

13. Saad, M.A. & Antonidest, G.J., "Flow Pattern of Two Impinging Circular Jets", AIAA Journal, 10, 1971, pp. 929-931.

14. Glauert, M.B., "The Wall Jet", Journal of Fluid Mechanics, 2, 1956, pp. 625-643.

15. Belotserkovskii, O.M., "Flow Past a Circular Cylinder with a Detached Shock Wave", Doklady Acad. Nauk. USSR, 113, 1957, pp. 509-516.

16. Chan, S.T.K., "Finite Element Analysis of Irrotational Flows of an Ideal Fluid", Ph.D. Thesis, University of California at Davis, 1971.

17. Norrie, D.A. & de Vries, G., "The LaPlace or Potential Field", The Finite Element Method - Fundamentals and Applications, Academic Press, New York, 1973, pp. 193-196.

18. Labus, T.L. & DeWitt, K.J., "Liquid Jet Impingement Normal to a Disk in Zero Gravity", Journal of Fluids Engineering, 100, 1978, pp. 204-209.

19. Strand, T., "On the Theory of Normal Ground Impingement of Axi-Symmetric Jets in Inviscid Incompressible Flow", AIAA Paper, No. 64-424, 1964.

20. Pollard, D.J. & Bradbury, L.J.S., "Impingement of a Two-Dimensional Supersonic Jet upon a Normal Ground Surface", AIAA Journal, 14, 1976, pp. 1095-1098.

21. Hrycak, P., "Heat Transfer from Impinging Jets, A Literature Review", Prepared under Grant NGR-31-009-004, Newark College of Engineering, Newark, New Jersey, 1968.

22. Tani, I. &Komatsu, Y., "Impingement of a Round Jet on a Flat Surface", Proc. XI, Int. Cong. of Appl, Mech., 1964, pp. 672-676.

23. Nogotov, E.F., "Applications of Numerical Heat Transfer", McGraw-Hill Book Company, 1978, pp. 7-56.

24. Saulyev, V.K., "Integration of Equations of Parabolic Type by the Method of Nets", Pergamon Press, 1964, pp. 29-82.

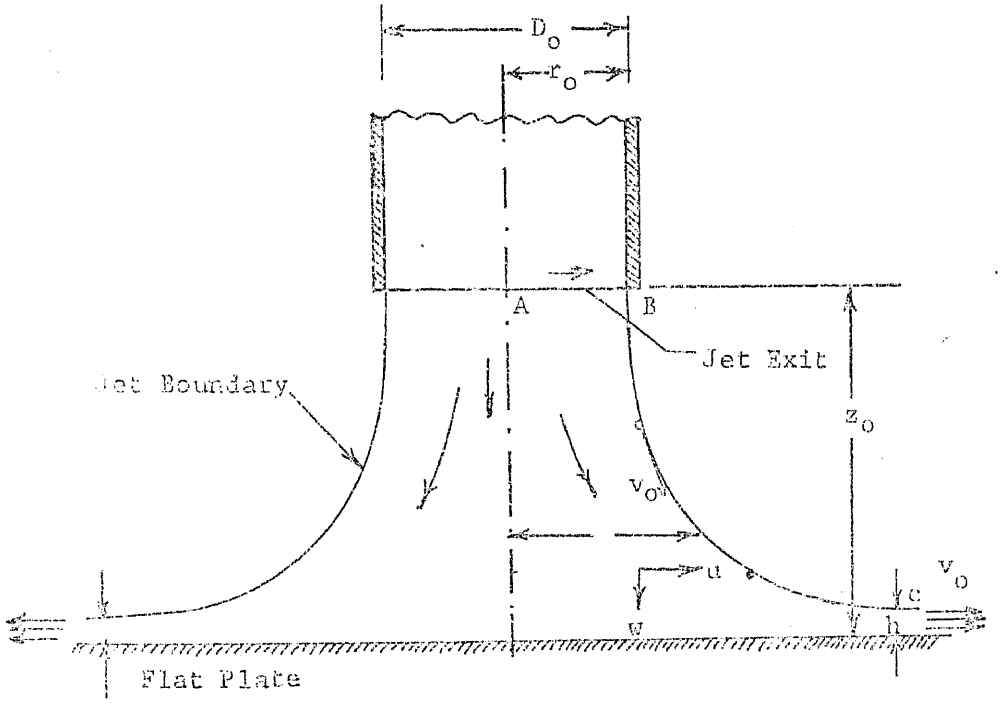

Flow Model for Circular Axi-Symmetric Jet Impinging on a Flat Plate.

Figure 1

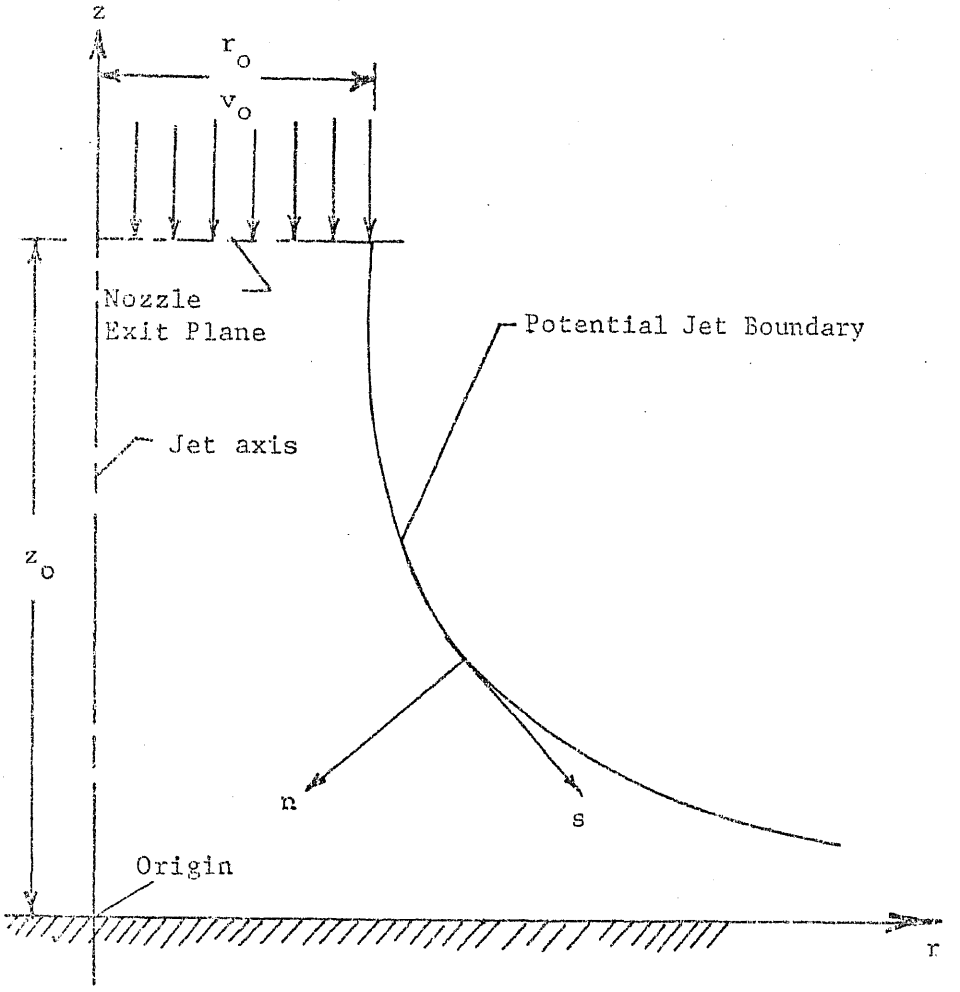

Graphical Representation of the Nomenclature
for the Impinging Jet.
Figure 2

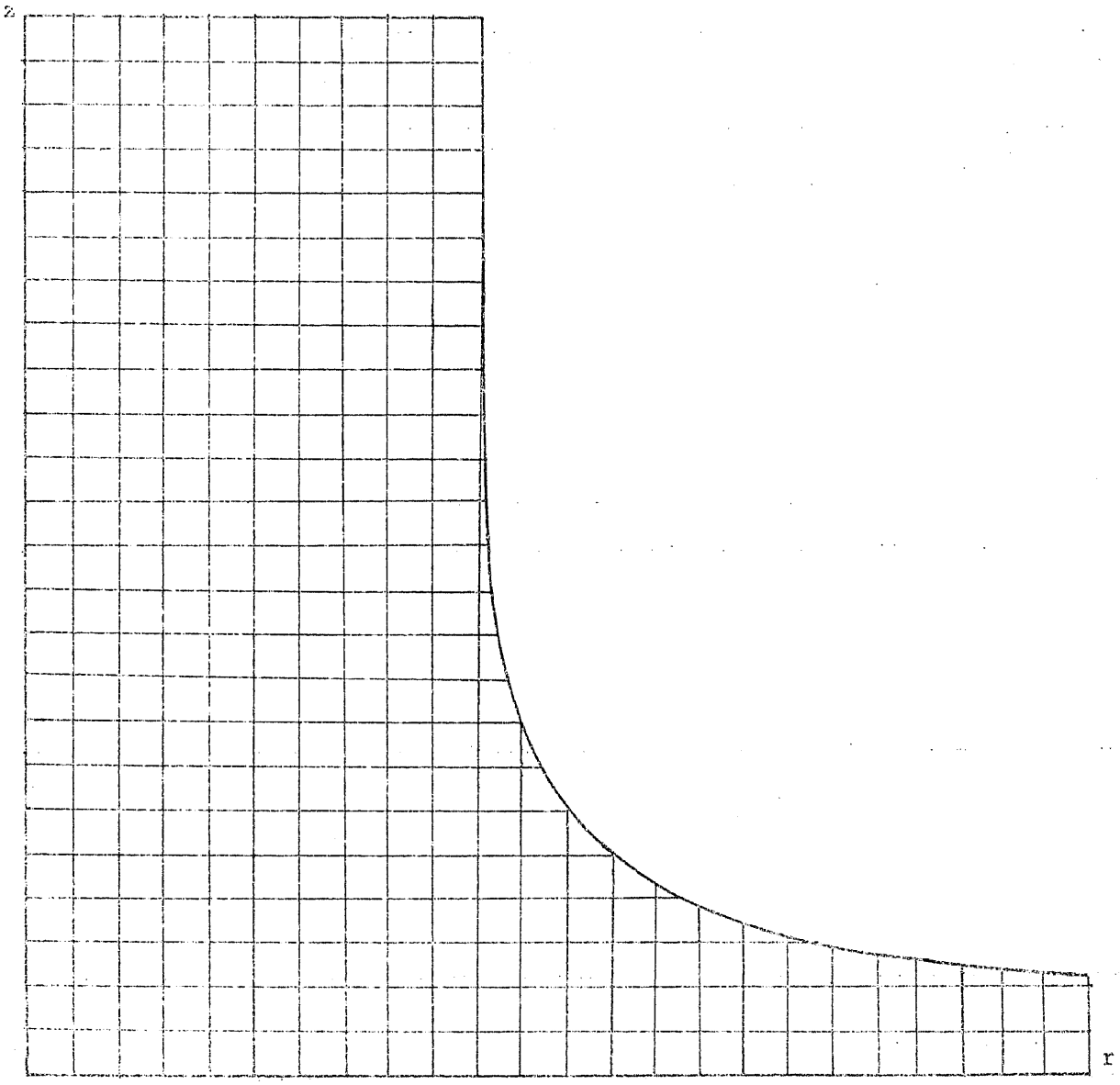

Finite-Difference Representation of an
Axisymmetric Jet Impinging on a Flat Plate.

Figure 3

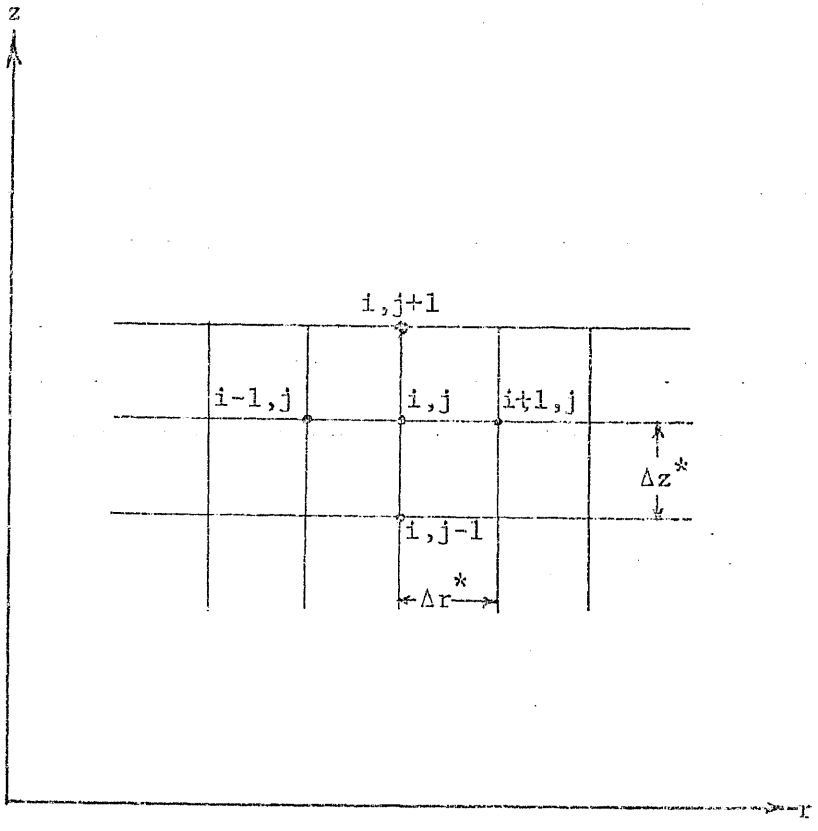

Grid Pattern for the Finite-Difference Solution of the Potential Flow Equation.

Figure 4

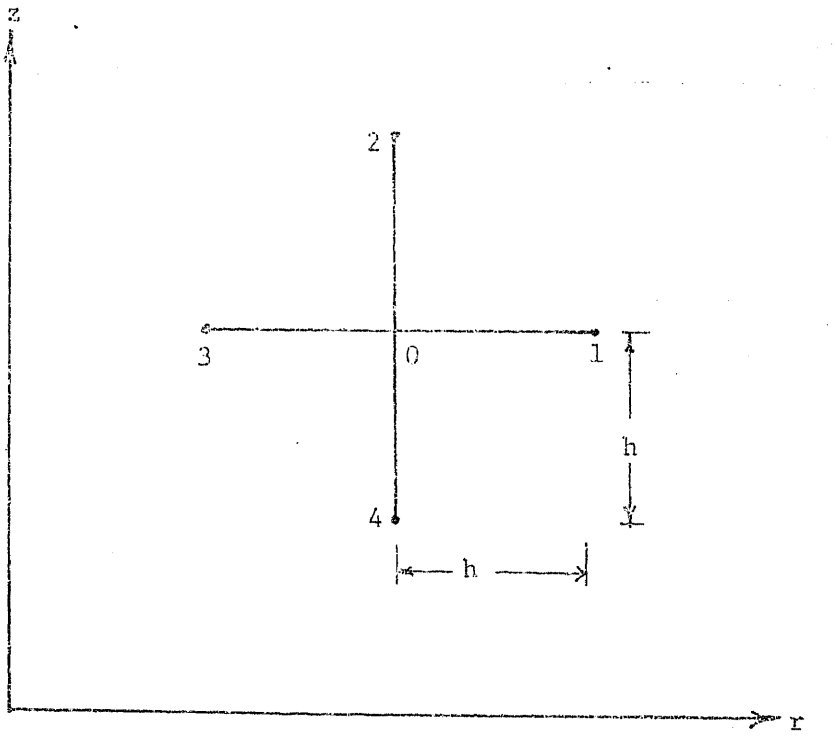

a: regular square mesh

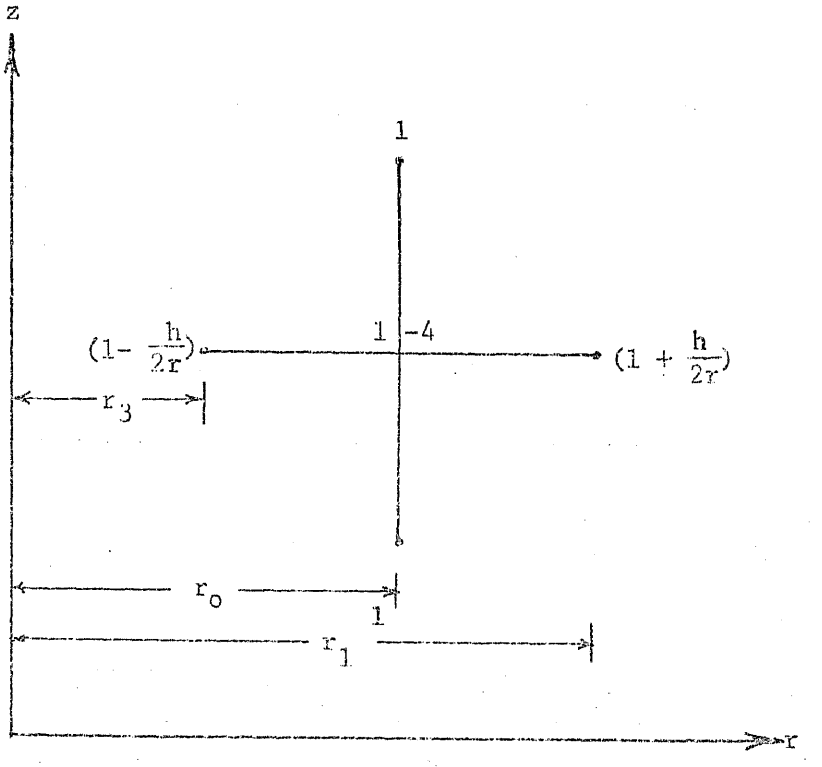

b: Laplace operator mesh

Figure 5

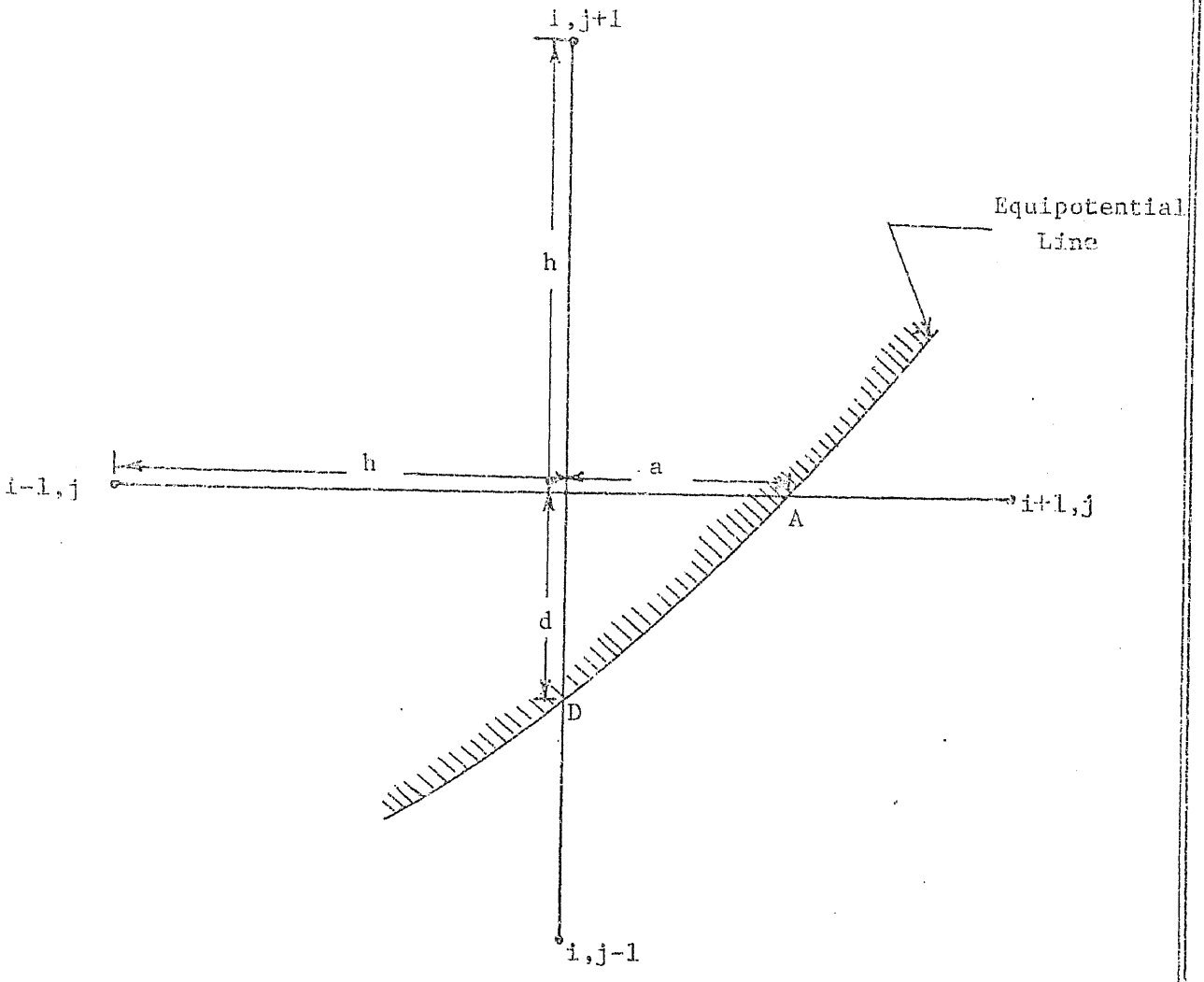

Node Notation with One Equipotential Line
Intercepting Two Mesh Lines.

Figure 6

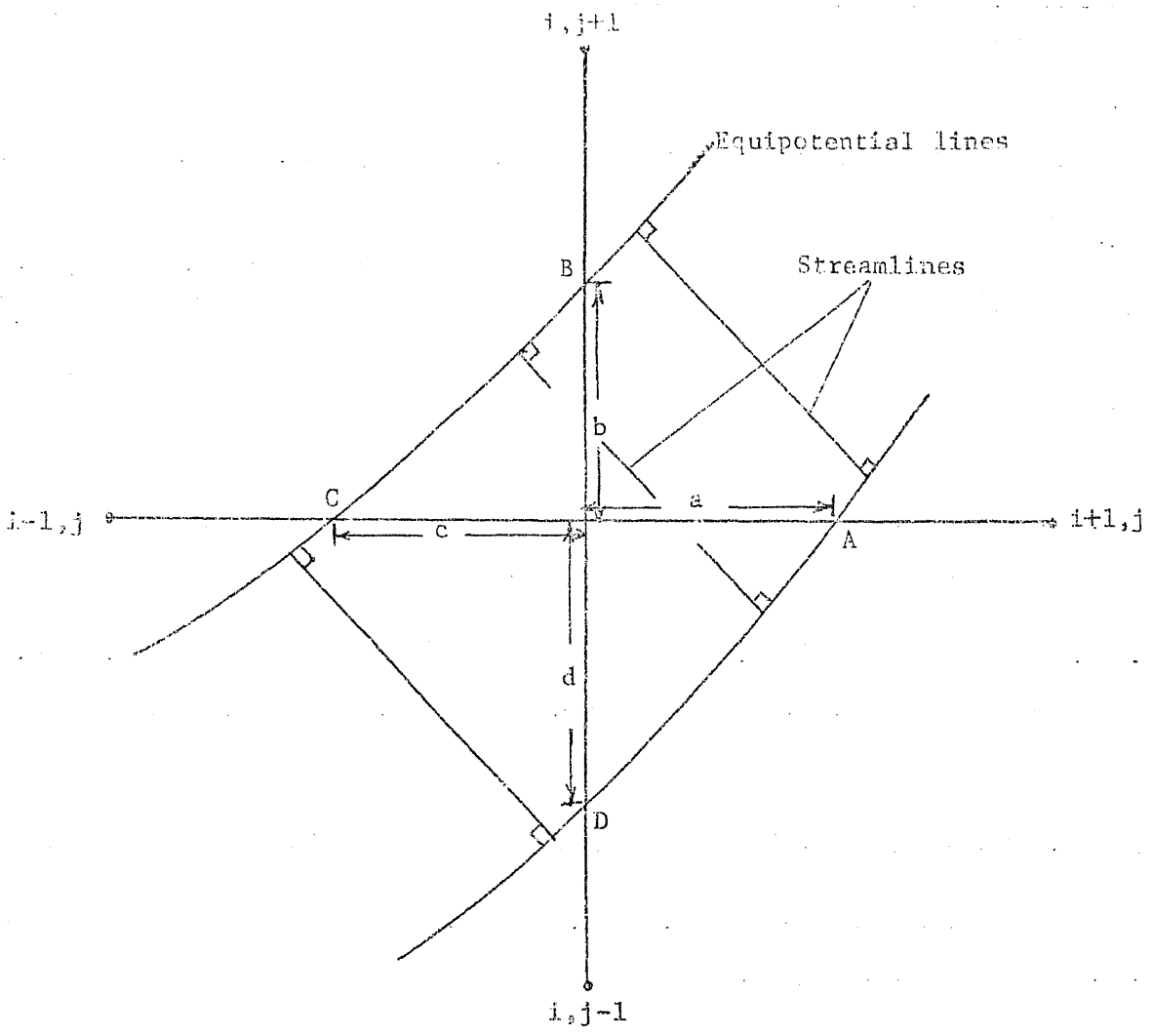

Node Notation with Two Equipotential Lines
Intercepting All Four Mesh Lines.

Figure 7

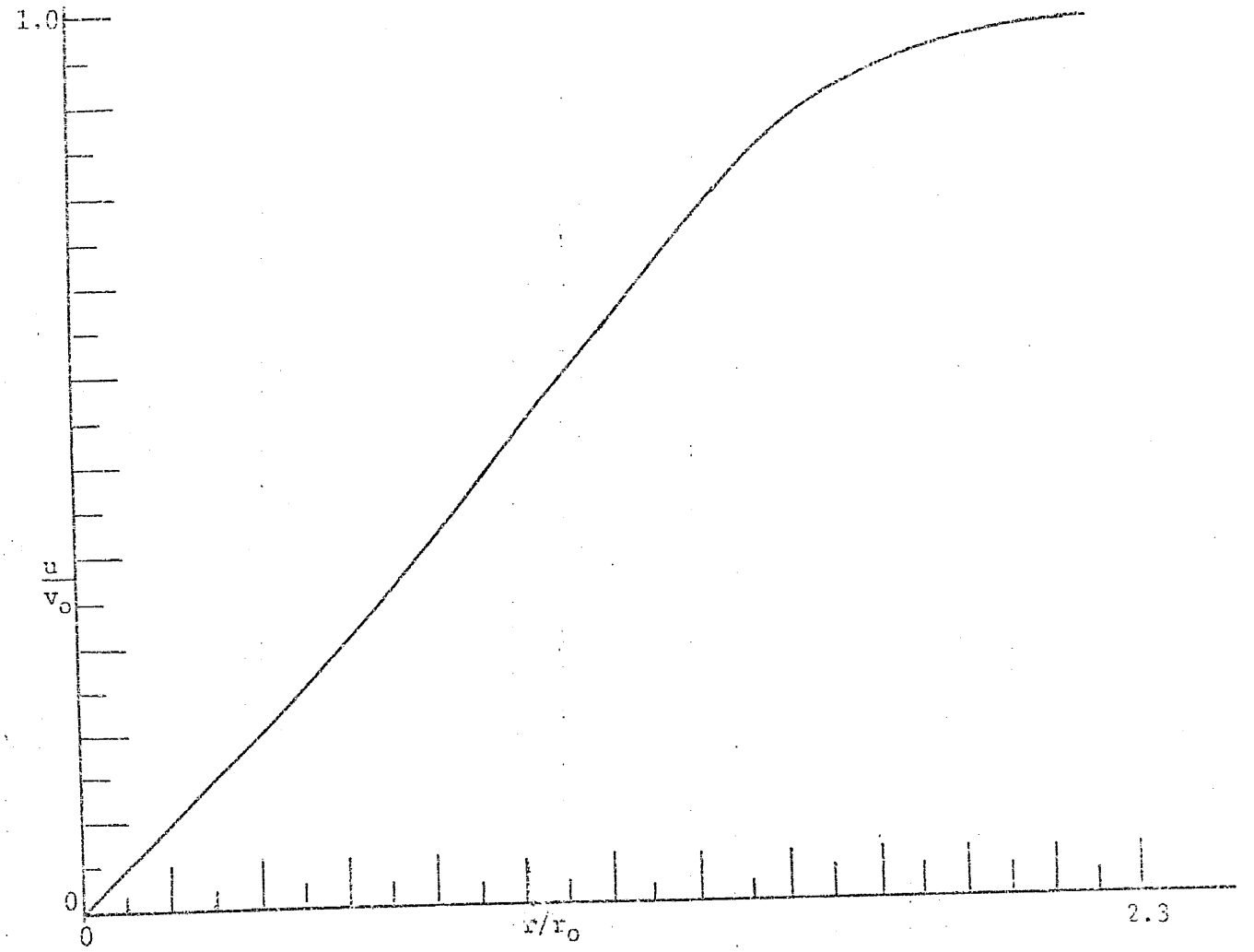

Velocity Distribution Along Flat Plate Surface.

Figure 8

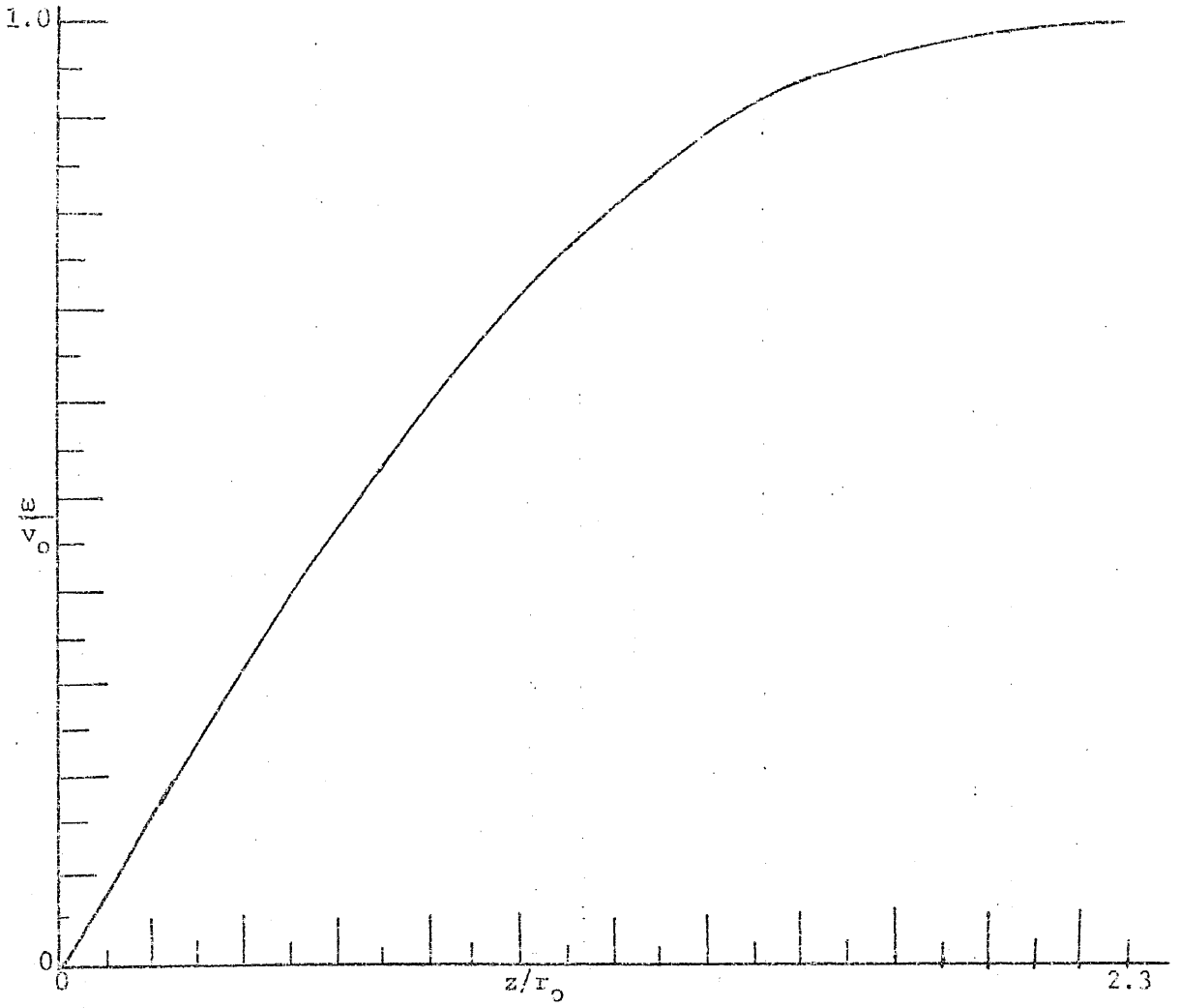

Velocity Distribution Along Jet-Centerline.

Figure 9

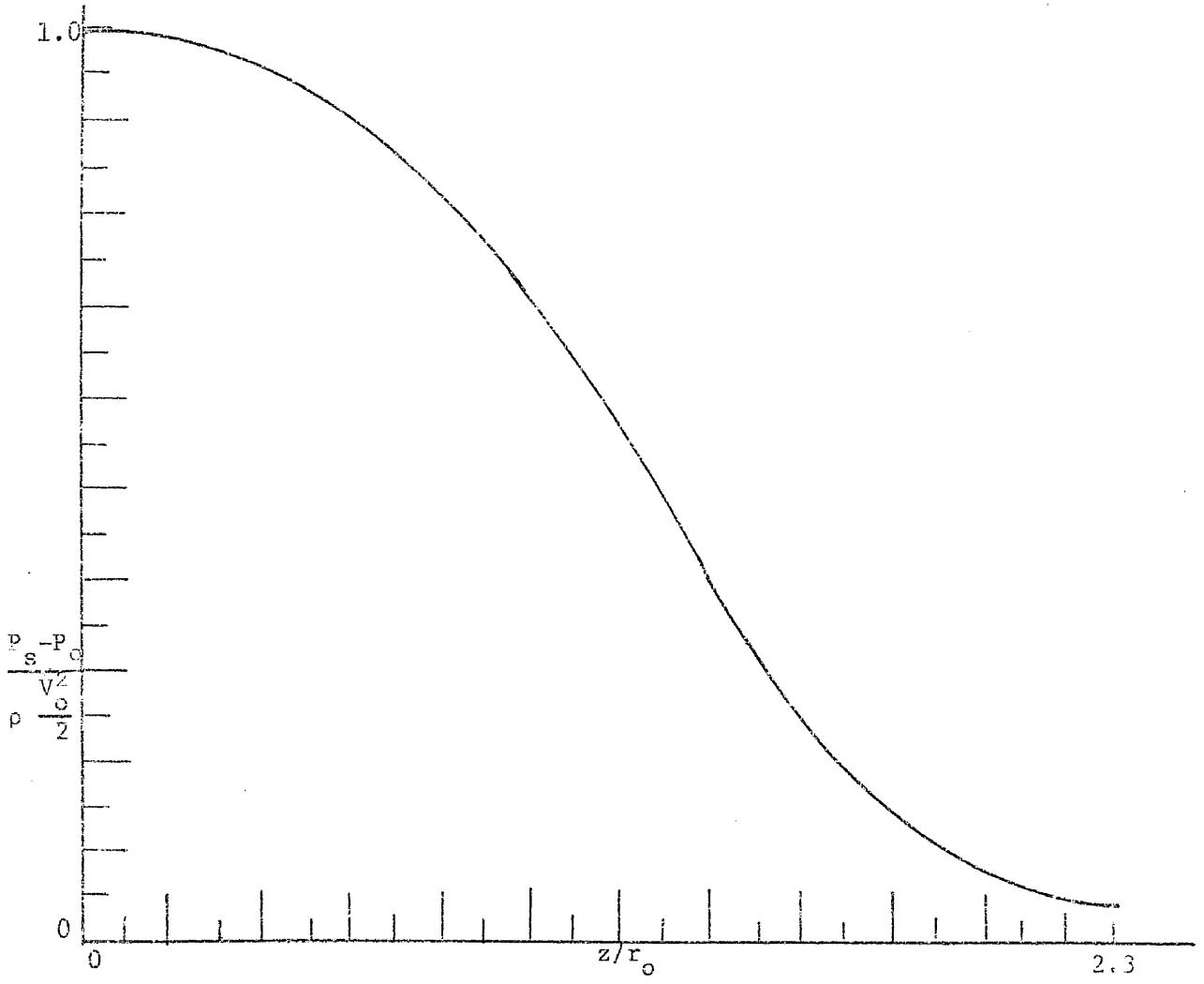

Static Pressure Distribution Along Flat Plate Surface.

Figure 10

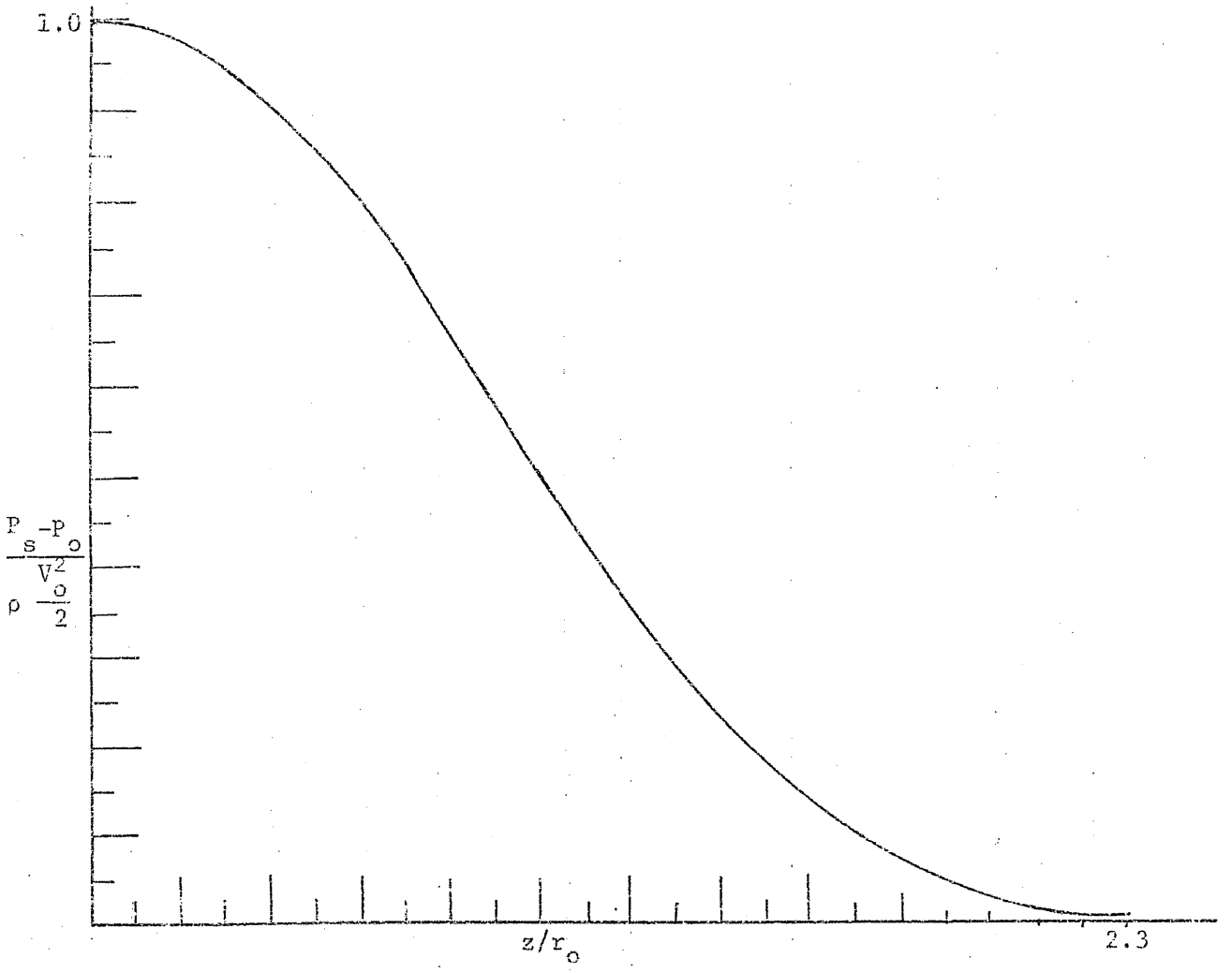

Static Pressure Distribution Along Jet-Centerline

Figure 11

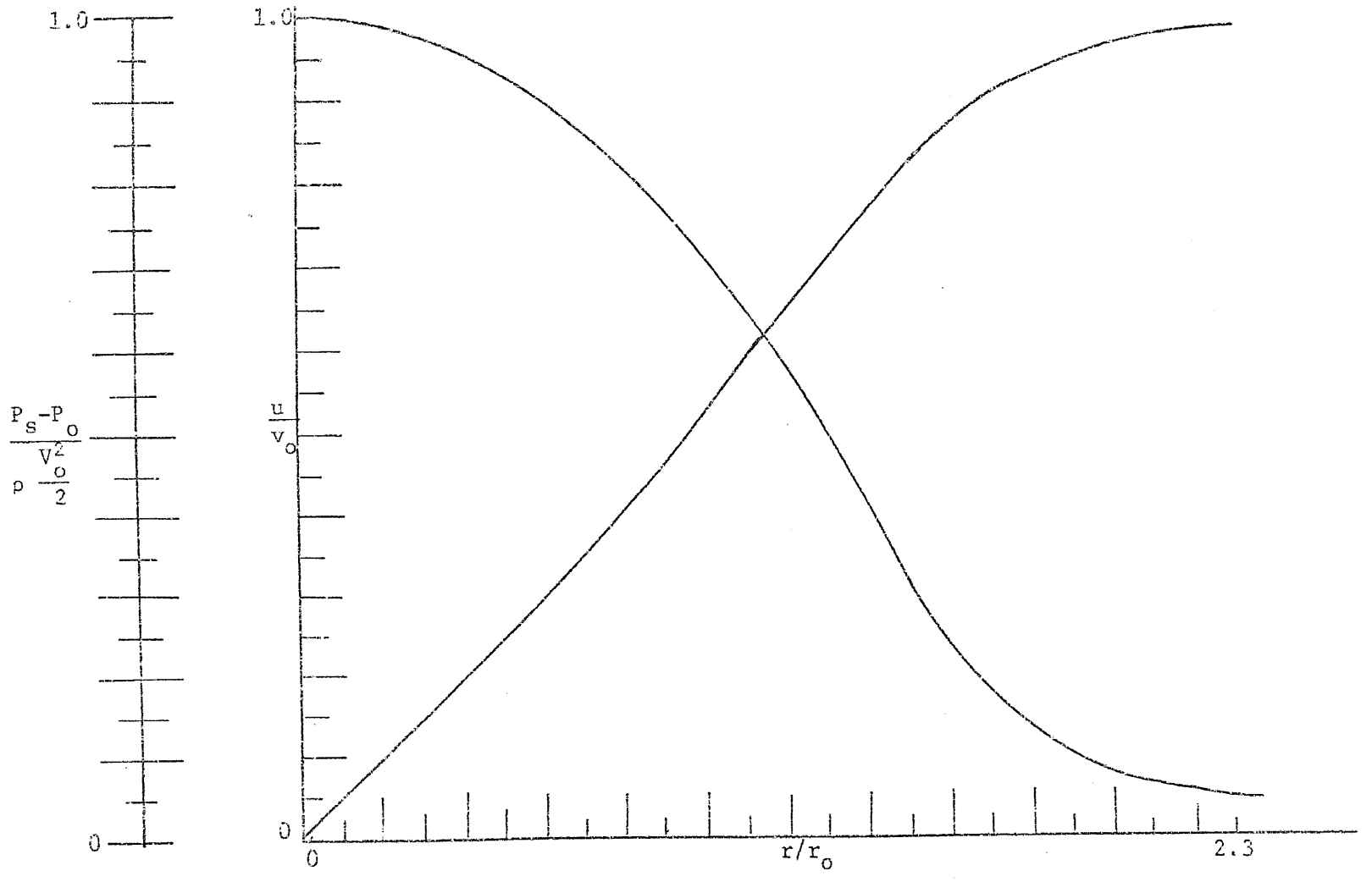

Radial Velocity and Pressure Distribution of an Axisymmetric Jet Impinging Upon a Flat Plate With a Height-to-Nozzle Radius Ratio of 2.4.

Figure 12

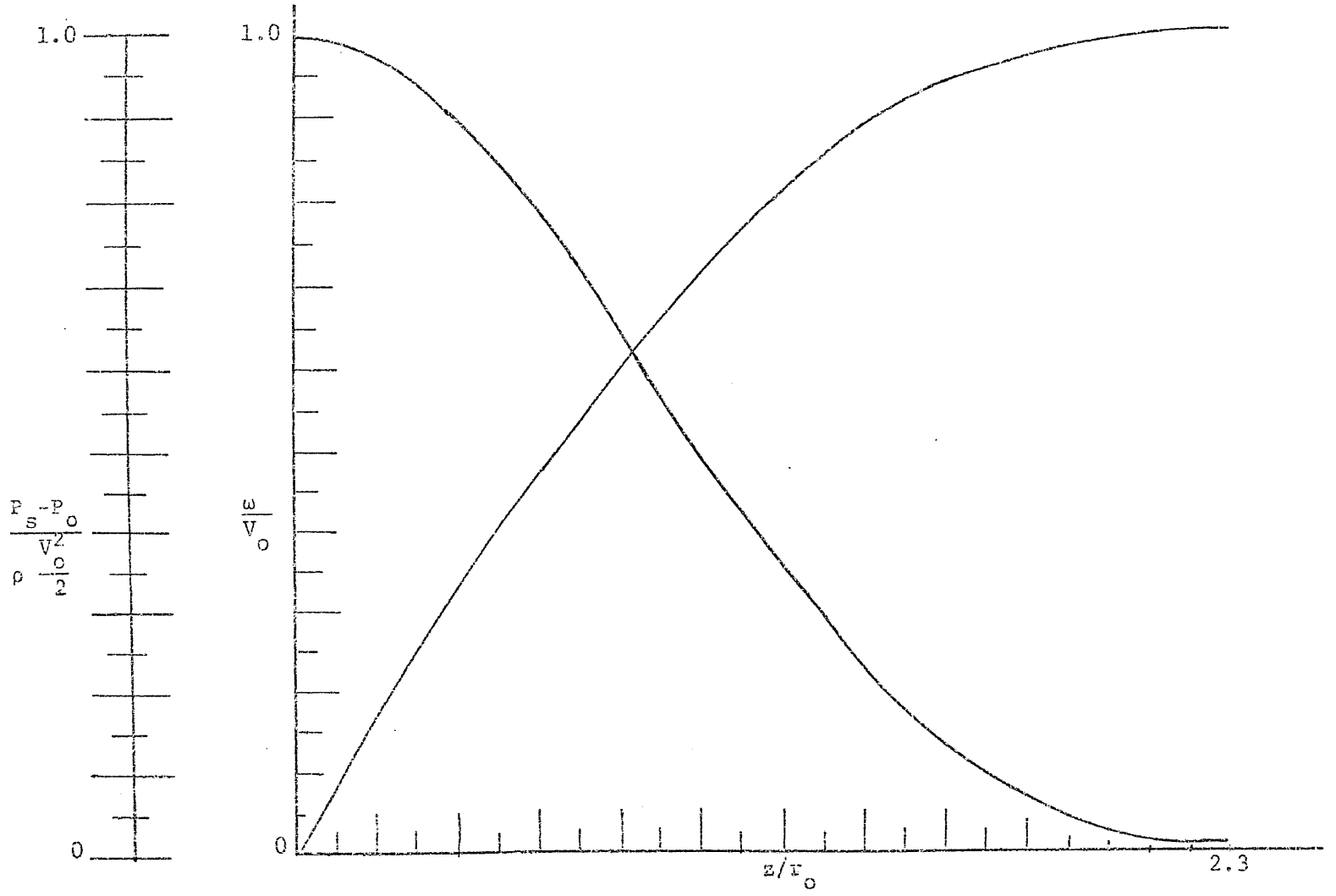

Axial Velocity and Pressure Distribution of an Axisymmetric Jet Impinging Upon a Flat Plate With a Height-To-Nozzle Radius Ratio of 2.4.

Figure 13

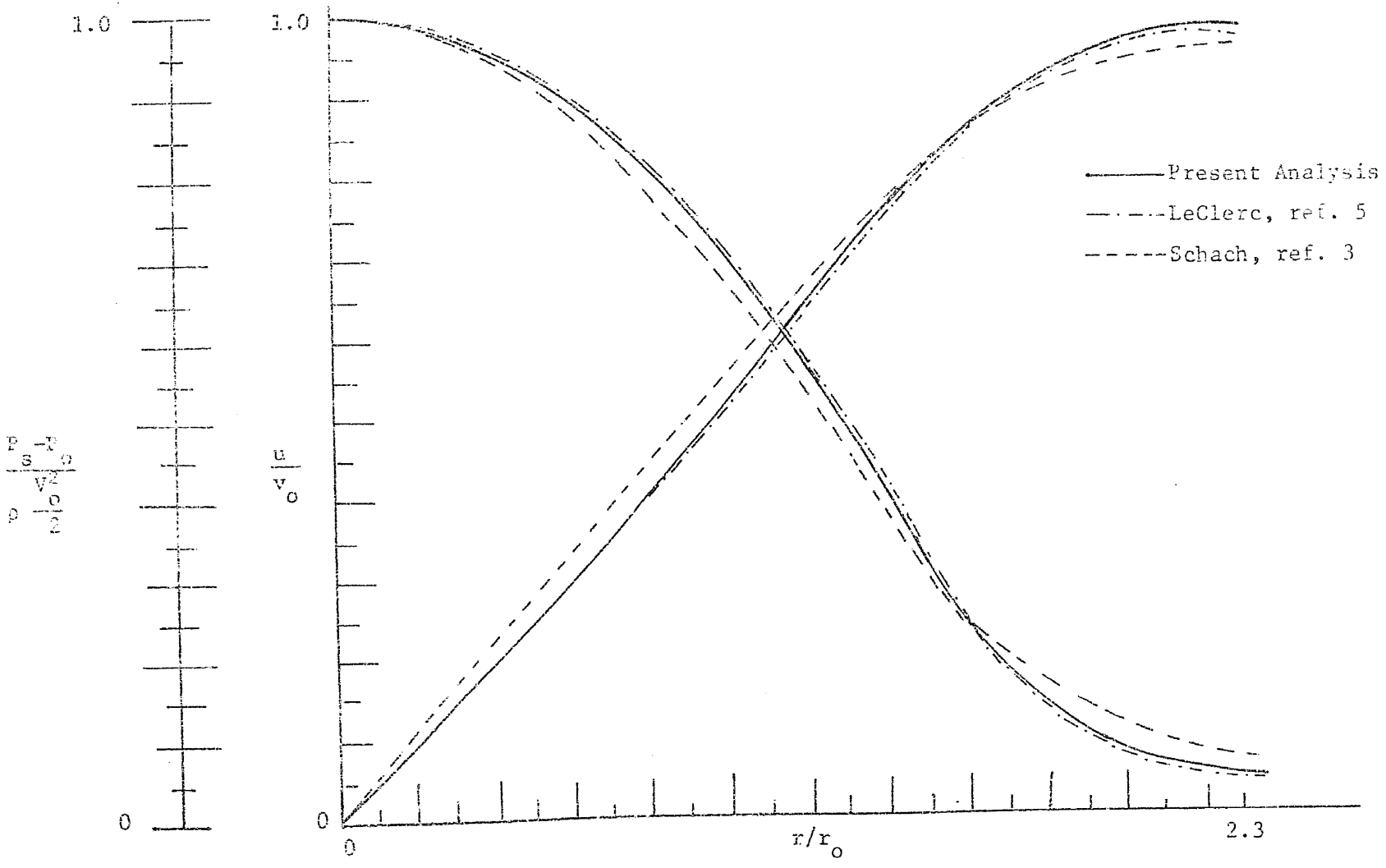

Comparison of Predicted Radial Velocity and Ground Plane Static Pressure Distributions of an Impinging Jet With a Height-To-Nozzle Radius Ratio of 2.4.

Figure 14

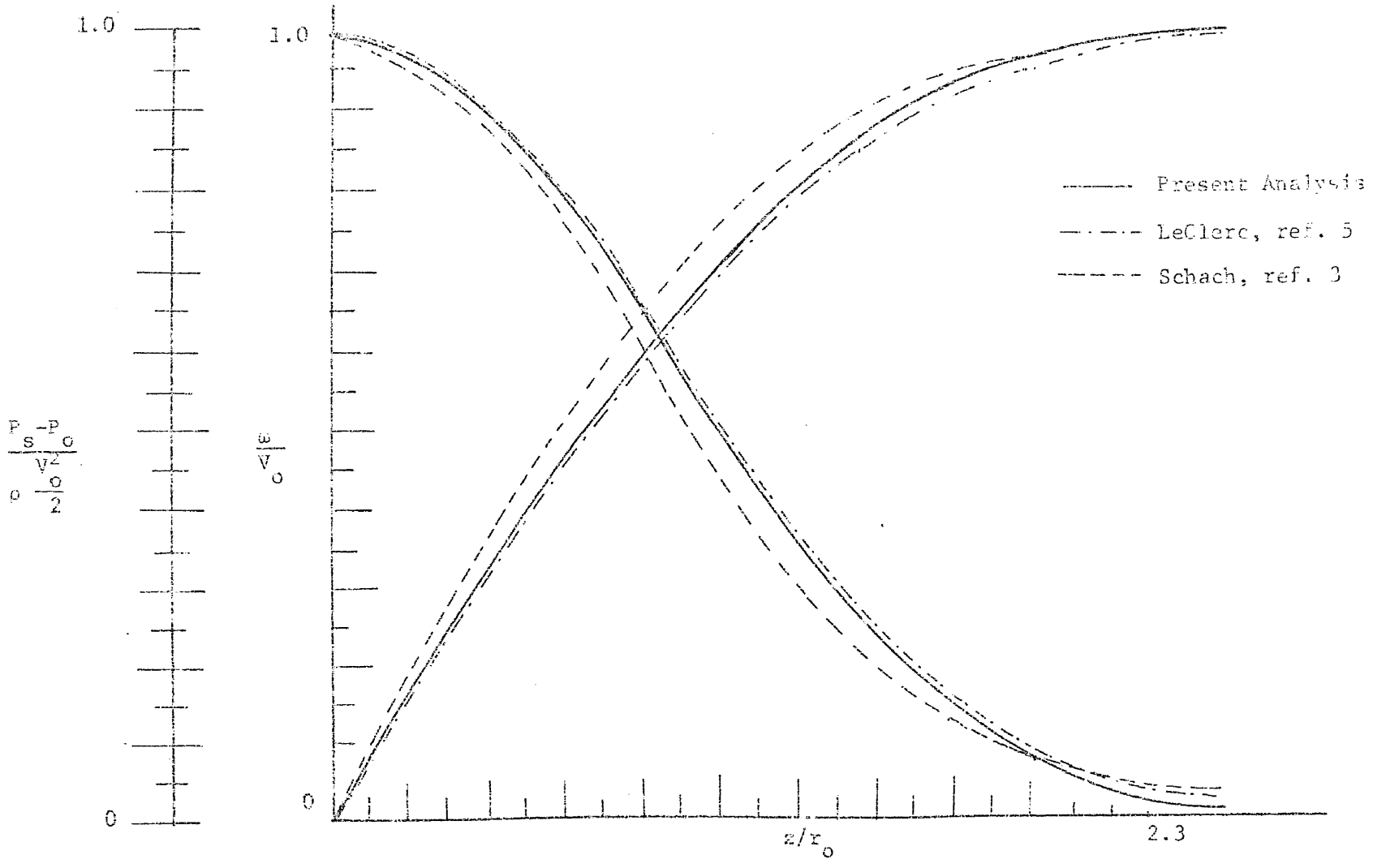

Comparison of Predicted Centerline Velocity and Static Pressure Distributions of an Impinging Jet with a Height-To-Nozzle Radius Ratio of 2.4.

Figure 15

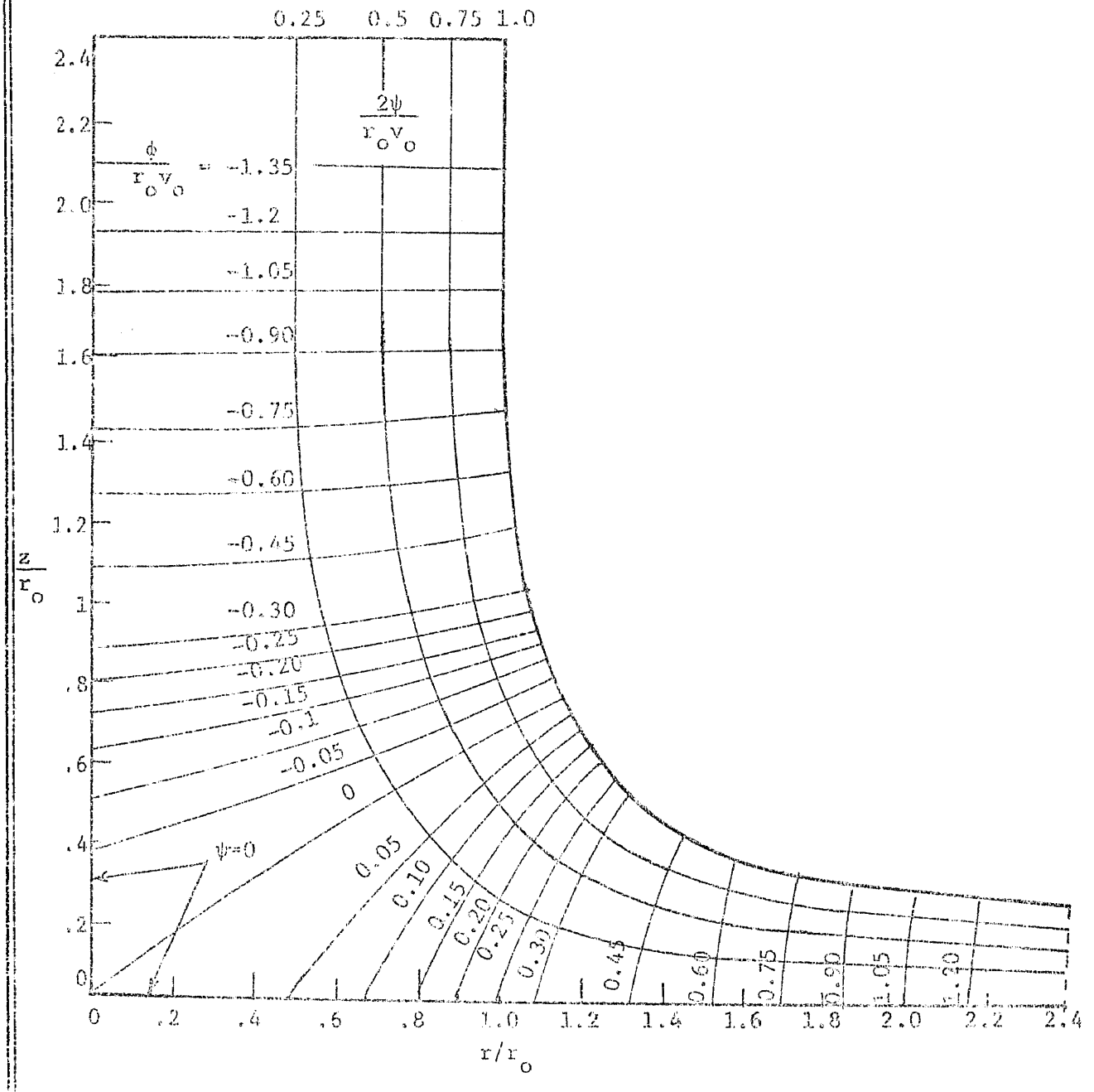

Flow Pattern of an Axisymmetric Jet Impinging Upon a Flat Plate

Figure 16